universität wien

MASTERARBEIT / MASTER'S THESIS

Titel der Masterarbeit / Title of the Master's Thesis

„The impact of restrictive diets on the gastrointestinal tract of mice "

verfasst von / submitted by

Laura Huber, BSc

angestrebter akademischer Grad / in partial fulfilment of the requirements for the degree of

Master of Science (MSc)

Wien, 2021 / Vienna, 2021

Studienkennzahl lt. Studienblatt / degree programme code as it appears on the student record sheet:	A 066 838
Studienrichtung lt. Studienblatt / degree programme as it appears on the student record sheet:	Ernährungswissenschaften
Betreut von / Supervisor:	Dr. techn. Kalina Duszka

Acknowledgement

There are so many people that made this master thesis possible, especially my friends and family. I know I cannot thank you all here, but to all the ones I did not mention by their name and who supported me on that journey so incredibly. Thank you!

Foremost, I would like to thank Dr. Kalina Duszka. Without your direct request, I would not sit here and write the last pages of my thesis. You taught me how experiments are built up in practice and what is important in the laboratory. You gave me the freedom to work on my experiments alone, and when I needed help or advice, you were always there for me. And as I often said: “When Kalina cannot help, who else?!” Thank you for empowering and teaching me so much in that short time, not only for my master thesis but also for my later life. You showed me, there is always a way how things will work. The benefit of this work goes far beyond the final thesis from the master.

Second, and equally important, I want to thank Univ.- Prof. Dr. Jürgen König. Without your permission it would have not been possible for me to do my master thesis in your working group. Thank you for being a part of your team!

Moreover, I want to thank Andras. You helped me a lot, especially with questions in the lab. Thank you for the time you invested in me. You also changed my view on snails. I already miss them. It was always great fun with you in the lab.

Lastly, I want to thank our companion cOVID-19 at this point. You and your mutants made it possible that I could focus on the lab and on my thesis with a minimum of distraction. Without you, I would not have appreciated it that much to go to the lab and work there.

Eidesstattliche Erklärung

Hiermit versichere ich, dass ich die vorliegende Masterarbeit selbstständig verfasst und keine anderen als die angegebenen Quellen und Hilfsmittel benutzt habe. Alle Ausführungen, die fremden Quellen wörtlich oder sinngemäß entnommen wurden, sind kenntlich gemacht.

Wien, am …

_____

Laura Huber

Index of Abbreviations

#	Strong trends (p=0,0071 to p=0,05)
*	Statistically significant differences (p>0,0071)
Acryl/Bis	Acrylamide/bis-solution 30
ADF	Alternate day fasting
APS	Ammonium peroxodisulfate
ATG	Autophagy-related protein
C10	Capric acid
C8	Caprylic acid
CNTRL	Negative control
CR	Caloric restriction
CTL	Control diet
ddH2O	Double destilled water
DNA	Deoxyribonucleic acid
Eef1a1	Eukaryotic translation elongation factor 1 α1
ELISAs	Enzyme-linked immunosorbent assays
EtOH	Ethanol
FMD	Fasting mimicking diet
fw	Forward
GSTA3	Glutathione S-transferase 3
H&E	Hematoxylin and eosin staining
IF	Intermittent fasting
IkBα	Nuclear factor kappa B inhibitor α
IKK	IkB kinase
IL	Interleukin
IBD	Inflammatory bowel disease
Keto-1	Ketogenic diet 1
Keto-2	Ketogenic diet 2

Keto-CTL	Ketogenic control diet
LCT	Long-chain triacylglycerol
M cells	Microfold cells
MCT	Middle-chain triacylglycerol
MGST1	Microsomal glutathione S-transferase 1
mRNA	Messenger ribonucleic acid
NCD	Non communicable disease
NF-kB	Nuclear factor kappa B
p	P-value
PAMPs	Pathogen associated molecular patterns
PBS	Phosphate-buffered-saline
PF	Periodic fasting
PFA	Paraformaldehyde
POS	Positive control
qRT-PCR	Quantitative real-time polymerase chainreaction
rv	Reverse
SDS	Sodium laurylsulfate
std	Standard
TBS	1x electrophorese buffer
TBST	0.1% Tween-20 in 1x TBS
TEMED	N, N, N’, N’-tetramethylenediamine
TRF	Time restricted feeding

Table of Content

Figures

Tables

1 Abstract

Food as the body's fuel have an enormous impact on the body. The way of eating and type of food triggers inflammatory pathways. Restrictive diets gained interest for its promising impact on health- and lifespan. Many beneficial effects such as a decrease in obesity, a reduction of inflammation and diseases, longevity, improvements in mood and cognitive tasks, as well as neuroprotective effects have been described already. Mouse studies showed the great impact of restrictive diets on the health status. However, most of the studies were conducted on sick mice and did not compare the effects of the diets together in one experiment on healthy individuals to figure out which diet has the greatest potential to decrease inflammation and increase health- and lifespan.

For the examination of different restrictive diets on inflammation markers and morphological changes in the gastrointestinal tract, healthy male C57Bl6 mice were divided into seven groups of eight mice receiving following diets: control diet (CTL), caloric restriction (CR), intermittent fasting (IF), fasting mimicking diet (FMD), ketogenic diet 1 (Keto-1), ketogenic diet 2 (Keto-2) and ketogenic control diet (Keto-CTL). In addition to histological examinations, the focus was also placed on the microbiota composition, autophagy processes and the antioxidative and immune response. Included in the study design were the examination of nuclear factor kappa B inhibitor α (IkBα), the cytokine expression, the glutathione S-transferase 3 (GSTA3) and microsomal glutathione S-transferase 1 (MGST1) and the autophagy related genes 7 and 12 (ATG7 and ATG12) expression in the small intestine epithelium tissue. Furthermore, the relative abundance of *Lactobacillus*, *Bacteroidetes*, *Firmicutes*, *Streptococcus* and *Deferribacter* in the feces were determined, as well as the changes in the morphology in the small intestine and colon.

The results showed that restrictive diets had an anti-inflammatory impact on the gastrointestinal tract of mice. Thereby, CR, IF, FMD and Keto-1 group were associated with the greatest reduction in inflammation markers.

Overall, restrictive diets showed promise in improving gastrointestinal health by altering the composition of the microbiota as well as gastrointestinal tissue and its cell function in an anti-inflammatory way. Nutrition works on many different levels in the body. Optimizing daily dietary composition and patterns could have a long-term and health-promoting impact on optimizing health span and preventing diseases.

Zusammenfassung

Die Nahrung als Treibstoff des Körpers hat einen enormen Einfluss auf den Körper. Die Art des Essens und die Art der Nahrung lösen Entzündungsprozesse aus. Restriktive Diäten haben aufgrund ihrer vielversprechenden Auswirkungen auf die Gesundheit und die Lebenserwartung an Interesse gewonnen. Viele vorteilhafte Effekte wie eine Abnahme der Fettleibigkeit, eine Reduzierung von Entzündungen und Krankheiten, Langlebigkeit, Verbesserungen der Stimmung und kognitiver Aufgaben sowie neuroprotektive Effekte wurden bereits beschrieben. Studien an Mäusen zeigten den großen Einfluss von restriktiven Diäten auf den Gesundheitszustand. Die meisten Studien wurden jedoch an kranken Mäusen durchgeführt und verglichen nicht die Auswirkungen der Diäten in einem Experiment an gesunden Individuen, um herauszufinden, welche Diät das größte Potenzial hat, Entzündungen zu verringern und die Gesundheits- und Lebenserwartung zu erhöhen.

Für die Untersuchung verschiedener restriktiver Diäten auf Entzündungsmarker und morphologische Veränderungen im Gastrointestinaltrakt wurden gesunde männliche C57Bl6-Mäuse in sieben Gruppen zu je acht Mäusen aufgeteilt, die folgende Diäten erhielten: Kontrolldiät (CTL), kalorische Restriktion (CR), intermittierendes Fasten (IF), Fasten mimicking diet (FMD), ketogene Diät 1 (Keto-1), ketogene Diät 2 (Keto-2) und ketogene Kontrolldiät (Keto-CTL). Neben histologischen Untersuchungen standen auch die Zusammensetzung der Mikrobiota, Autophagie-Prozesse sowie die antioxidative und Immunantwort im Fokus. In das Studiendesign eingeschlossen waren die Untersuchung des Nuclear Factor Kappa B Inhibitor α (IkBα), der Zytokinexpression, der Glutathion-S-Transferase 3 (GSTA3) und der mikrosomalen Glutathion-S-Transferase 1 (MGST1) sowie der Expression der Autophagie-bezogenen Gene 7 und 12 (ATG7 und ATG12) im Dünndarmepithelgewebe. Darüber hinaus wurden die relative Häufigkeit von Lactobacillus, Bacteroidetes, Firmicutes, Streptococcus und Deferribacter im Kot sowie die Veränderungen der Morphologie im Dünn- und Dickdarm bestimmt.

Die Ergebnisse zeigten, dass die restriktive Diät eine entzündungshemmende Wirkung auf den Gastrointestinaltrakt der Mäuse hatte. Dabei waren CR, IF, FMD und die Keto-1-Gruppe mit der größten Reduktion der Entzündungsmarker verbunden.

Insgesamt zeigten restriktive Diäten ein vielversprechendes Ergebnis bei der Verbesserung der gastrointestinalen Gesundheit, indem sie die Zusammensetzung der Mikrobiota sowie das gastrointestinale Gewebe und seine Zellfunktion auf entzündungshemmende Weise veränderten. Die Ernährung wirkt auf vielen verschiedenen Ebenen im Körper. Die Optimierung der täglichen Nahrungszusammensetzung und -muster könnte einen langfristigen und gesundheitsfördernden Einfluss auf die Optimierung der Gesundheitsspanne und die Prävention von Krankheiten haben.

2 Introduction

2.1 Restrictive diets

Depending on the diet, the metabolism changes. One way of changing it is through food restriction. Food restriction enables the organism to develop alternative metabolic phases, which rely more on fat and ketone bodies and less on glucose [77]. Under normal physiological conditions, glucose is the primary substrate for energy. However, when glucose is sparse, for example during restrictive diets, fat and ketone bodies can serve as energy source. Ketone bodies are mainly produced out of fat and proteins and depend on low insulin levels for their production, which enhance lipolysis, the breakdown of fats. The produced ketone bodies acetoacetate, ß-hydroxybutyric acid and acetone are transported through the bloodstream to the peripheral cells, where they are converted to acetyl-CoA and metabolized into energy in the mitochondria [13, 64]. Ketones show a neuroprotective effect by enhancing the brain's energy metabolism. These effects were already proved in neurodegenerative diseases, where the glucose metabolism in the brain was declined [54].

Fasting can be defined as a voluntary reduction of or abstinence from some or all food, drinks, or both for a certain period lasting generally between 12 hours and 3 weeks. This could be executed in form of short term, long term or an intermittent fasting pattern [100]. Fasting is not only known in the religious context but also for its health benefits and its potential for longevity. At this point it is important to separate fasting from starvation. Starvation is a chronic and strong caloric deficiency below the level needed for maintaining a healthy life [69]. Fasting however is based on a negative energy balance, that results in achieving weight loss, as well as many other health benefits [69].
Another way to enhance the metabolic pathway of ketone bodies is through ketogenic diets. The ketogenic diet is based on a high fat and low-carbohydrate diet which mimics the metabolic state of long-term fasting by forcing the body to use fat instead of carbohydrates as its major source of energy [32].

In the following chapters, different restrictive diets are listed.

2.1.1 Caloric restriction

CR is based on a reduction of daily calorie intake. Common are restrictions between 20 to 40%, but also stricter ones, higher than 50% are performed [7]. CR was associated with a reduction in oxidative and inflammatory stress [5]. Previous studies showed that CR prevented several inflammatory [84] and chronic degenerative diseases, prolonged life in primitive species including yeast and Escherichia coli [93] and had positive effects on the mood [83]. The high life expectancy in the Okinawan population in Japan was associated at least in part with a lower calorie intake compared to the mainland [126]. Currently, CR is regarded as the gold standard for many aging intervention methods. Although it is well researched that CR has

many positive effects in counteracting aging processes, the exact mechanisms are still controversial [16].

2.1.2 Intermittent fasting

Intermittent fasting (IF) is a form of fasting that consists of cycles between fasting and non-fasting periods. It is an umbrella term including alternate-day-fasting (ADF), time restricted feeding (TRF), and periodic fasting (PF). ADF means fasting on one day and eating *ad libitum* on the next day. TRF is based on a restriction of the time where the individual can eat during a day. An example of periodic fasting is the 5:2 diet, meaning two fast days during a week. In previous studies IF showed already a great impact on health. It was associated with a reduction of inflammation and diseases, an increase in stress resistance, longevity, and a reduction of obesity. Moreover, previous studies showed IF affected directly the composition of the gastrointestinal microbiota, their function and the interaction with the host [11, 58, 73].

2.1.3 Fasting mimicking diet

Through the understanding of some connections between nutrients, fasting and the benefits for the metabolism, the development of compounds that mimic the effects of CR are of great interest [113]. Prof. Longo developed a method, namely fasting mimicking diet (FMD), which achieves similar changes to those caused by fasting. FMD is characterized by undergoing periodic cycles of fasting. Compared to IF and CR, FMD provides a relatively high calorie content. It mimics the beneficial effects of fasting by decreasing the proportion of visceral fat, reducing inflammatory diseases, decreasing bone mineral density loss and leading to improvements in cognitive tasks [77].

2.1.4 Ketogenic diets

Ketogenic diets were developed in the 1920s, as a treatment for epilepsy, based on observations on the positive impact of this diet on the anti-seizure effect of epileptic attacks [63]. The interest in ketogenic diets and other ketogenic treatments has proliferated during the last decade. Ketone bodies are now used not only for epileptic treatments but also as a potential therapeutic strategy in several diseases such as diabetes, cardiovascular diseases, cancer and neurodegeneration [38, 87].

The classic ketogenic diet comprises a 4:1 ketogenic ratio of fat compared to combined carbohydrates and protein. Most dietary fat consists of so called long-chain triacylglycerol (LCTs). However, medium-chain triacylglycerol (MCTs) are more ketogenic, meaning they produce more ketone bodies per unit of energy compared to LCTs [48, 140]. LCTs require a transporter for entry into the mitochondrial matrix, where they are converted into acetyl-CoA. That is a limiting step for the ketosis during ketogenic diets. Compared to LCTs, MCTs do not rely on a transporter protein for entry into the mitochondria [33].

Ketogenic diets showed a positive impact on neurological diseases like epilepsy [89, 140], Alzheimer's disease [19], Huntington disease [96], amyotrophic lateral sclerosis [121] and Parkinson's disease [139]. One common feature in neurodegenerative diseases is the disruption of the energy metabolism in the brain, meaning a hypometabolism of glucose in affected brain regions which correlates to the severity of the disease [19, 96, 121, 139]. Ketogenic diets support the brain's energy supply via an additional pathway besides glucose and can slow down the progression of diseases or even prevent the onset of diseases if the diet is started early enough [20].

2.2 The gastrointestinal microbiota

Hippocrates said 2500 years ago what the science is proving nowadays "all disease begins in the gut". The microbiome plays an important role in maintaining health. Relations between the gastrointestinal microbiota and human health are being increasingly recognized. The gastrointestinal microbiome has a substantial functional plasticity and an extensive metabolic capability [78]. It consists of estimated 2,000 different species and corresponds to approximately a weight of 1.5 kilograms. The intestinal microbiome plays an essential part in the digestion. Not only are important micronutrients and vitamins produced there, but the microbiome also influences the motility of the colon [114]. It maintains a symbiotic relationship with the gastrointestinal mucosa by imparting substantial immunological, metabolic, and gastrointestinal protective functions in the individual. The maintenance of the structural integrity of the mucosal barrier protects the individual from pathogen colonization [52, 134]. One of the major activities of the microbiota is to break down substrates such as resistant starch and dietary fiber, which are incompletely hydrolyzed by host enzymes in the small intestine. The primary fermentation products resulting from fiber breakdown are the short-chain fatty acids (SCFAs) acetate, propionate and butyrate, which provide an additional source of energy for the body [110]. Disruptions of the gastrointestinal microbiota, referred to as gut dysbiosis, is commonly observed in human diseases ranging from obesity and diabetes [26] to colorectal cancer [134], neurodevelopmental illnesses, as well as allergic [56] and inflammatory gastrointestinal diseases [47, 71]. Since non-communicable diseases (NCDs) show a strong increase nowadays, more and more studies are focusing on the role and changes in the composition of microbiota in the gastrointestinal tract.

The healthy human gastrointestinal microbiota comprises two major phyla, namely *Firmicutes* and *Bacteroidetes* [52, 131]. *Bacteroidetes* is a primary degrader of polysaccharides in the gastrointestinal tract [66]. A decrease in the population was in previous studies associated with obesity [72] and chronic inflammatory skin diseases [118]. An abundance of *Bacteroidetes* was associated with a decrease in LDL-Cholesterol [92].
The bacteria *Firmicutes* supports fat absorption. Previous studies associated an increase of *Firmicutes* population with obesity [50, 81, 105]. Therefore, these two bacteria were combined to form the Firmicutes/Bacteroidetes ratio as a biomarker for obesity. However, due to significant variability even in healthy individuals, the relationship is not completely reliable so far [50, 81].
Another core microbe is *Parasutterella*. Same as *Bacteroidetes* and *Firmicutes*, it has been

identified as a healthy fecal core microbiome member in the human gastrointestinal tract [127]. *Parasutterella* produces succinate as fermentative end product [94]. Results using a germ-free mouse model showed that bacterially produced succinate stimulated the colonization of anaerobic bacteria, which protected mice from infection [61]. Therefore, *Parasutterella* may play an important role in microbial interactions and resistance of infections.
The abundance of *Deferribacter* was in previous studies associated with inflammatory metabolic pathways. An increase of these bacteria has been linked to type 2 diabetes [92] and higher expression of interleukin (IL)-1ß. An increase of *Deferribacter* could therefore contribute to an overexpression of inflammatory cytokines, especially in the colonic mucosa [68].
The bacteria *Lactobacillus* is best understood and known for its essential role in food fermentation and probiotic applications. Although the bacteria are only minor members of the colonic microbiota, they have a great impact on health. Several animal studies showed a connection between *Lactobacillus* and the prevention of infectious diseases and recovery of immune homeostasis [30, 43, 57, 133]. A depletion of the amount of *Lactobacillus* in the intestine was associated with prenatal stress [35, 138], type 1 diabetes [1, 34], multiple sclerosis [15, 115], irritable bowel syndrome [75], and human deficiency virus (HIV) [122, 130]. Enriched levels were associated with Crohn's disease [70, 124] and rheumatoid arthritis [76, 136]. In obesity [24, 46, 49, 67, 105], type 2 diabetes [31, 59], and colorectal cancer [10, 41] the levels of *Lactobacillus* were either enriched or depleted.
Another member of the gastrointestinal microbiome is *Streptococcus*. An abundance of these bacteria was in previous studies associated with low grade inflammation in the knee [9] and chronic skin diseases [99].

2.3 Structure of the gastrointestinal barrier

One way to study the effects of different restrictive diets on the gastrointestinal tract is to examine the morphology of the intestine. The intestinal barrier is the separation of the body and its environment. To keep the body healthy, one needs a well-functioning intestinal barrier to prevent penetrations of foreign substances and pathogens. The intestinal mucosa is also the central lock for nutrients, vitamins, electrolytes, and trace elements. These substances must be able to pass through the intestinal barrier to reach the interior of the body and supply all body cells.

From the outside looking in, the intestinal barrier consists of the following components:

2.3.1 The mucus

The mucus consists of two layers: an inner layer, which adheres firmly to the epithelial cells, and an outer layer, which is about twice as thick, much looser, and less adherent. The inner, dense layer keeps bacteria away from the epithelial layer, while the upper layer provides a habitat for the intestinal microbiome. The function of the mucus goes far beyond a simple

barrier. It contains glycans, which serve as food for the bacteria and are probably also involved in the selection of specific microbial species essential for maintaining integrity, homeostasis and digestion [95].

2.3.2 The intestinal mucosa

The intestinal mucosa consists of a single layer of different polarized cell types which form a physical barrier between body and the environment. The small intestinal mucosa is organized in many crypt-villus units. Villi are finger like protrusions of the gastrointestinal wall which project into the gastrointestinal lumen to maximize the absorptive surface area. A villus is covered by an epithelium, and underneath are capillaries and lymph vessels that mediate the transport of absorbed nutrients into the body. The villus is surrounded by epithelial invaginations, called crypts of Lieberkühn. The crypts contain proliferating epithelial cells, that fuel the active process of self-renewal of the epithelium.
The intestinal mucosal epithelium is built of different cell types. The most populous cells are enterocytes. Enterocytes handle the absorption of different substances from the food. They are tall cells with an apical surface with microvilli called luminal brush border that further increases the absorptive area of a villus. Another common cell type in the mucosal barrier are goblet cells. These cells are rounded at the end and secret mucus, which builds a protective layer for the mucosal epithelium. Neuroendocrine (enteroendocrine) cells secrete various hormones and Paneth cells secrete bactericidal peptides such as defensins and lysozymes. Compared to goblet cells and neuroendocrine cells which both occur on the villi intestinalis and in crypts, Paneth cells are placed only on the bottom in the crypts. Microfold (M) cells are cell of the immune system. They reside in the Peyer`s patches, a lymphoid accumulation, which plays a key role in the mucosal immunity [18, 107].

All the cells of the intestinal mucosa are connected via tight junctions. Tight junctions are protein connection between the epithelial cells of the intestinal mucosa. They are crucial for the tightness of the intestinal barrier. Besides their barrier function, the tight junctions form a kind of fence between the apical and basolateral proteins of the cell membrane. In this way, the fence strictly separates the proteins on the top and bottom of the cell and thus maintains the polarity of the epithelial cells [108].

Below the intestinal mucosa there are also several other cells of the innate and adaptive immune systems stationed, which are involved in integrity on the one hand and in inflammatory reactions on the other. The intestinal mucosa-associated lymphoid tissue contains up to 70 percent of the immune cells of the entire human body. Here it is decided which bacteria are tolerated and which are classified as dangerous and subsequently combated. This happens through the contact of the bacteria with specific immune cells such as the dendritic cells and the M-cells within the Peyer's patches [101].

Under the mucosa is the submucosa, the muscularis externa and the adventitia.

The cross-sectional structure of small intestine epithelium tissue and its major cell constituents is shown in the figure below.

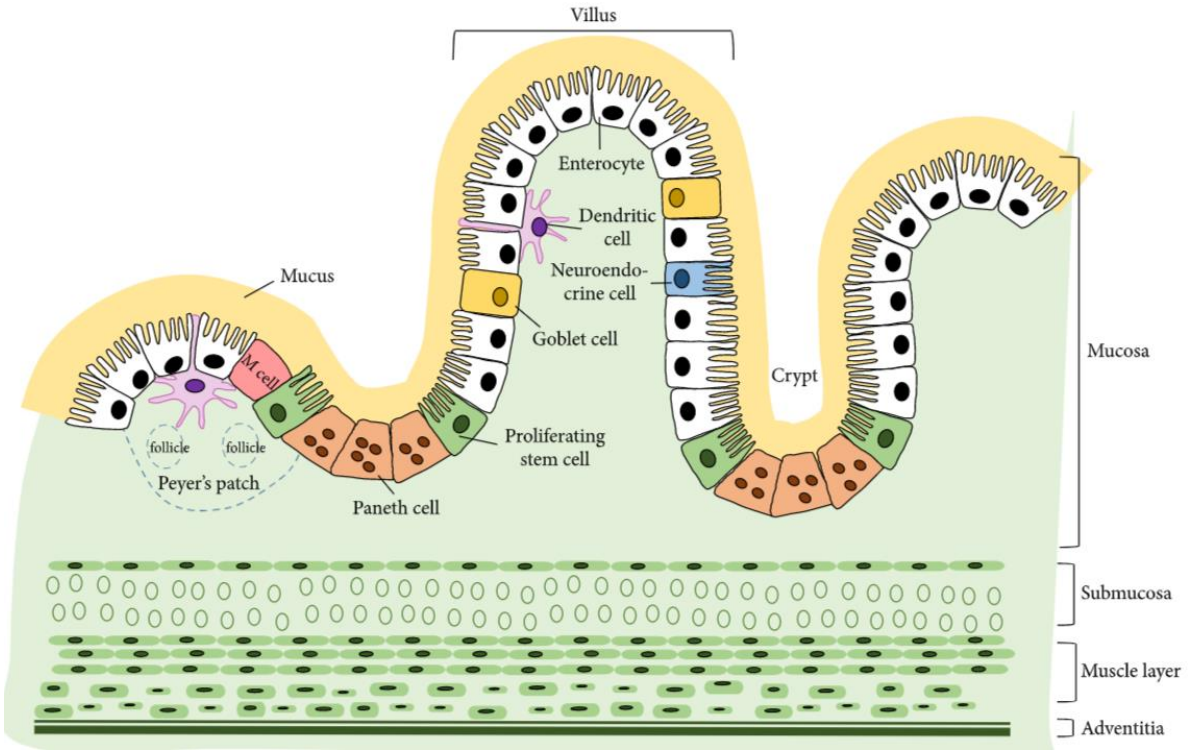

Figure 1:Cross-sectional structure of small intestine epithelium tissue and its major cell constituents [62]

Small intestine epithelium tissue consists of villi intestinalis and crypts, while epithelium tissue in the colon only of crypts. The schematic illustration shows the differences between these two tissues.

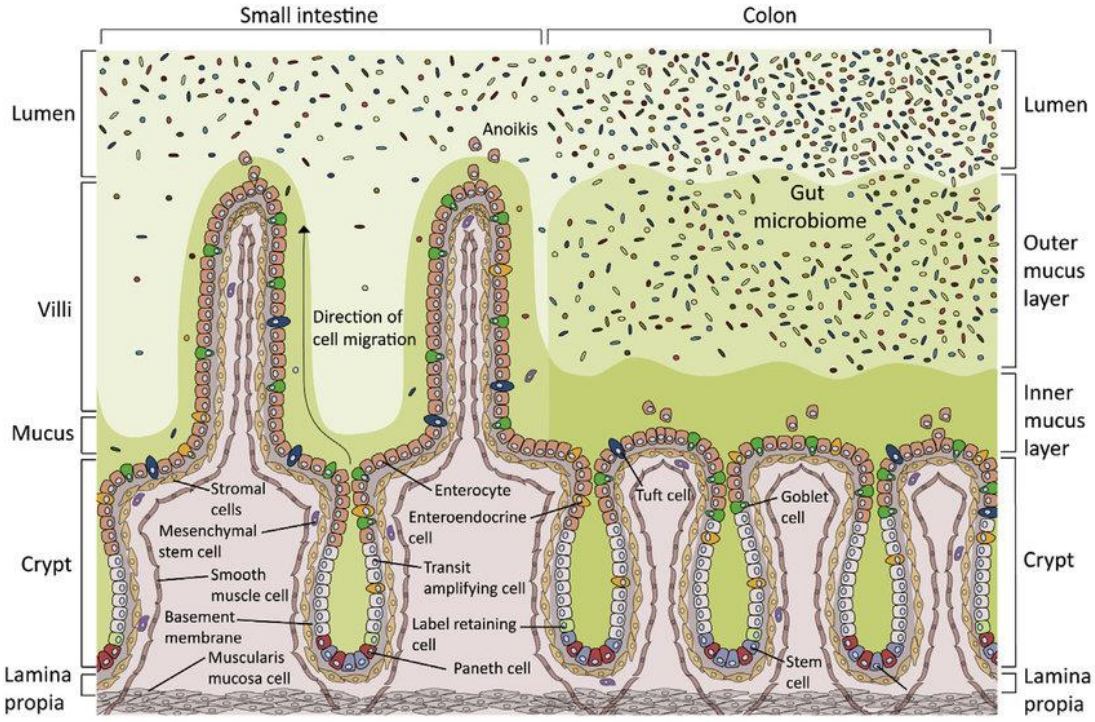

Figure 2:The structure of the small intestine and colon epithelium [27]

In the mid-1990s, scientists discovered that the epithelial cells of the intestine can adapt their phenotype under changing conditions and produce proinflammatory mediators such as cytokines [25]. This happens, for example, when pathogenic bacteria cross the mucus layers and encounter the epithelial cells.

2.3.3 Restrictive diets and their impact on the goblet cells

Similar to the increasing number of microbiota in the intestine, the proportion of goblet cells raises from duodenum (4%) to distal colon (16%) [60]. In a previous study it was shown, that fasting increased the number of duodenal goblet cells by 25%, but did not change the number of these cells in the other gut segments. In fasted-refed rats, the number of goblet cells in duodenum and colon was increased [28].

2.3.4 Restrictive diets and their impact on the villi intestinalis and crypts

Fasting shows an effect on the cell proliferation in the intestine. The nutrient availability affects the intestinal epithelial stem cell proliferation and tissue growth. Previous studies showed, that an increase in food amount resulted in a greater number of epithelial cells, height of villi intestinalis and depth of crypts [6]. In another study, a decrease of 30% in mitosis in the crypts during fasting was observed [37]. Inflammation in the gastrointestinal tract is characterized by reduced villous length and crypt depth, atrophy and disruption [17, 104, 123, 129].

2.3.5 Restrictive diets and their impact on the muscularis externa

The muscularis externa comprises two layers of smooth muscle, the inner layer called circularly oriented layer and the outer layer called longitudinally oriented layer. Between the connective tissue is the myenteric plexus, also called Auerbach's plexus. This plexus contains ganglion cells, a kind of nerve cells and lymphatic vessels and blood vessels [107]. Alteration in the muscularis externa may be caused by an activation of macrophages and a following release of chemokines and cytokines that causes an inflammatory cell influx of neutrophilic granulocytes and mononuclear cells. In further consequence, the morphology and the homeostatic functionality of the muscularis externa changes [125]. An irreversible thickening of the muscularis externa was shown in induced Crohn's like disease in the colon in a rat model [116].

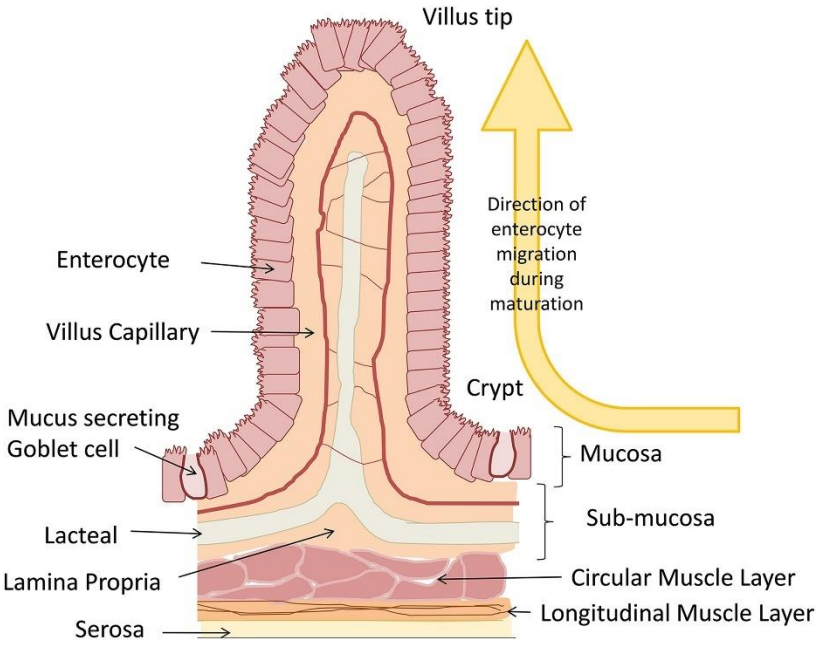

Figure 3: Generalized cross-section of intestinal villus along the crypt to villus tip axis [39]

2.4 Inflammation markers with emphasis on the gastrointestinal tract

2.4.1 NF-κB and its inhibitor IkBα

The family of nuclear factor kappa B (NF-κB) transcription factors comprises five members, namely NF-κB1 (p50), NF-κB2 (p52), RelA (p65), RelB and c-Rel, which form homo- and heterodimers. In the absence of specific stimuli, these dimers are bound to IκB, the inhibitor of NF-kB and kept transcriptionally inactive. The NF-κB signaling pathway responds to different patterns, from growth factor signaling and cytokines to the recognition of DNA damages and pathogen products. To activate NF-κB, it induces the formation of IκB kinase (IKK) protein complex. IKK leads to a phosphorylation of IκBα and consequently to its detachment from NF-κB and degradation. The NF-κB dimers can now enter the nucleus where they regulate the transcription of their target genes [44, 45]. NF-κB is involved in activating inflammatory and immune responses but also in regulating autophagy, adhesion, angiogenesis, energy metabolism, senescence, as well as inducing cell proliferation and survival [42, 51, 119]. Previous studies described an increase of NF-kB, a decrease in IkBα, and an increase in the expression of proinflammatory cytokines by diverse inflammatory processes [5, 21, 86].

Also in the gastrointestinal tract, gut inflammation is associated with an increased production of proinflammatory cytokines, such as TNF-α, IL-1, and IL-18, that activate the NF-κB pathway in the gastrointestinal wall [29]. Previous studies described NF-κB as a key player in the inflammatory bowel disease (IBD) development. The level of activation of this transcription factor correlated with the severity of intestinal inflammation [2, 90, 91, 109]. A current study from Mikuda et al. showed that a deficiency in IκBα in the intestinal epithelium leaded to spontaneous inflammation and mediated apoptosis in the gastrointestinal tract [85].

2.4.2 Cytokines

Cytokines are small proteins which play a crucial role in innate immunity, angiogenesis, cell growth, differentiation, and apoptosis. They are important in physiology and in most diseases, especially in immune responses, inflammation, trauma, cancer, reproduction, sepsis, and host responses of infections. They are produced by endothelial cells and immune cells like macrophages in the muscularis externa [128]. Previous studies described a correlation between a decrease in IkBα and an increase in the expression of proinflammatory cytokines such as TNF-a, IL-1ß, IL-12 and IL-18 [5, 21, 86, 135].

2.4.3 GSTs

Glutathione S-transferases (GSTs) are enzymes which conjugate glutathione (GSH) to toxic metabolites or xenobiotics (18). The thiol-containing tripeptide GSH plays a major role in the anti-oxidative system in cells [82]. Increases in the oxidized form (GSSG) and decreases in the reduced form (GSH) are associated with an increase in oxidative stress [36, 53]. Formed conjugates of GSH and metabolites or xenobiotics can be removed from the metabolism by transport out of the cell and excretion or degradation. Therefore, GSTs play a central role in the detoxification of organic substances. GSTs are a diverse family of microsomal, mitochondrial, and cytosolic enzymes that prevent cellular damage from noxious stimuli of xenobiotic metabolites. These enzymes are widely present throughout the body and are abundant in liver, kidney, and lungs [40, 65, 102]. Accumulating evidence shows that GSTs also influence many biological mechanisms, such as signal transduction, redox homeostasis, cell proliferation, and cell death. These regulatory functions are exerted by activating or inhibiting the target molecules of pathways, such as c-Jun N-terminal kinases (JNK), apoptosis signal-regulating kinase 1 (ASK1), and NF-κB [8, 55, 117, 120].

Two members of GSTs are glutathione S-transferase 3 (GSTA3) and microsomal glutathione S-transferase 1 (MGST1). Genes of the alpha class, such as GSTA3, encode enzymes with glutathione peroxidase activity and are also involved in progesterone and testosterone biosynthesis. MGST1 is a representative of the MAPEG family. These proteins are found at the outer mitochondrial membrane and the endoplasmic reticulum (ER) to protect the membranes from oxidative stress [3, 4].

2.5 Autophagy with emphasis on ATG7 and ATG12

Autophagy is a well-defined process to either restore cellular homeostasis or initiate cell death through breaking down and utilizing components [137]. Under stress conditions, such as nutrient deficiency, autophagy is activated to promote cell survival and maintain well-working cell function. Previous studies associated the beneficial effects of CR with enhanced autophagy processes [80, 106], a dysregulation was associated with age-related diseases [16, 22, 23]. Two markers of autophagy are autophagy related gene 7 and 12 (ATG7 and ATG12). These two genes encode proteins that increase the activity. Therefore, they are conducive to cell homeostasis and cell survival [14, 132].

This master thesis was designed to give answer to the questions below.

Which impact have restrictive diets on the inflammation levels in the immune status in healthy mice? Can these diets lead to a reduction in inflammation? If yes, which diet is most effective in minimizing inflammation and therefore improving health?

3 Materials and Reagents

3.1 General materials

Centrifuge 5418R, 100 rpm – 14 000 rpm, 0°C to 40°C, Eppendorf Ltd. (Hamburg, Germany)

Centrifuge tubes; 15 ml, 50ml, Corning Ltd. (Corning, New York, USA)

Microcentrifuge tubes, 1.5 ml and 2.0 ml, Eppendorf Austria Ltd. (Vienna, Austria)

Pipette, Research plus; 2.5µl, 10µl, 20µl, 100µl, 200µl, 1000µl, Eppendorf Austria Ltd. (Vienna, Austria)

Tips TipOne®; 10µl, 200µl, 1000µl, STARLAB International Ltd. (Hamburg, Germany)

Vortex mixer, lab dancer, VWR® International Ltd. (Radnor, USA)

3.2 Materials for histological cuts

3.2.1 Equipment

Axiocam ERc 5s, Carl Zeiss Microscopy Ltd. (Göttingen, Germany)

Embedding station AP 250 W, Microm Ltd. (Walldorf, Germany)

GFL Paraffin stretching bath (1052), Lauda-GFL Ltd. (Burgwedel, Germany)

Microscope Axio Lab 5x H SF 22, Carl Zeiss Microscopy Ltd. (Göttingen, Germany)

Peltier-cooled incubator IPP110, VWR® International Ltd. (Radnor, USA)

Semi-motorized rotary microtome (RM2245), Leica Biosystems Ltd (Nussloch, Germany)

3.2.2 Softwares

Excel 2013 software

ImageJ processing program

Zeiss efficient Navigation Software Program (ZEN)

3.2.3 Accessories

Dyeing troughs for manual dyers (12 pieces), VWR® International Ltd. (Radnor, USA)

Histology cassettes, VWR® International Ltd. (Radnor, USA)

Low Profile Microtome Blades DB80 LS, Leica Biosystems Ltd. (Nussloch, Germany)

Micro cover glasses (20x20 mm)

Microscope slides (pre-cleaned/ready-to-use/ground edges) Superfrost® Plus, Thermo Scientific Ltd. (Braunschweig, Germany)

Slide holders, VWR® International Ltd. (Radnor, USA)

Slideboxes (100 lames), VWR® International Ltd. (Radnor, USA)

Stainless steel caps for dyeing troughs (12 pieces), VWR® International Ltd. (Radnor, USA)

3.3 Materials for western blot

3.3.1 Equipment

Analysing system ChemiDoc XRS+, Bio-Rad Laboratories Ltd. (Hercules, USA)

Color Sprout centrifuge Biozym Biotech Trading Ltd. (Vienna, Austria)

EU power cable IEC coupler C13/C14 220V, Bio-Rad Laboratories Ltd. (Hercules, USA)

Impulse welding machine PM-FS-200-S, Rotek Ltd. (Hagenbrunn, Austria)

MINI-P TETCOMP SYS10W1.0MM, Bio-Rad Laboratories Ltd. (Hercules, USA)

Mini Rocker-Shaker PMR-30, Grant-Instruments Ltd. (Shepreth, UK)

Power Pac HC Power Supply, Bio-Rad Laboratories Ltd. (Hercules, USA)

SpectraMax Me, Refurbished, Molecular Devices Ltd. (San Jose, USA)

Thermomixer 5436, Eppendorf Austria Ltd. (Vienna, Austria)

10 TGX Stain-Free Fast Cast Starter Kit, Bio-Rad Laboratories Ltd. (Hercules, USA)

Trans-Blot® TurboTM Transfer System, Bio-Rad Laboratories Ltd. (Hercules, USA)

3.3.2 Softwares

Image Lab™ software (5.0)

SoftMax Pro 7.0

3.3.3 Accessories

Filter paper 415, VWR® International Ltd. (Radnor, USA)

Immun-Blot® PVDF membranes for protein blotting, Bio-Rad Laboratories Ltd. (Hercules, USA)

Omnifix-F, 1 ml, Braun Melsungen Ltd. (Bad Arolsen, Germany)

Sterican (size 14), 0,60x30 mm, Braun Melsungen Ltd. (Bad Arolsen, Germany)

TC plate 96 well, suspension, Sarstedt Ltd. (Nümbrecht, Germany)

Tubular cover film, ALLPAX Ltd. & co. (Papenburg, Germany)

3.4 Materials for qRT-PCR

3.4.1 Equipment

CFX Connect Real-Time PCR Detection System, Bio-Rad Laboratories Ltd. (Hercules, USA)

3.4.2 Software

QuantStudio (TM) 6 Flex System

3.4.3 Accessories

384-well PCR plates, Thermo Scientific Ltd. (Rockford, USA)

innuPREP Stool DNA Kit from Analytik Jena Ltd. (Jena, Germany)

Omnifix-F, 1 ml, Braun Melsungen Ltd. (Bad Arolsen, Germany)

qPCR seal, 4titdue (Surrey, UK)

Sterican (size 14), 0,60x30 mm, Braun Melsungen Ltd. (Bad Arolsen, Germany)

3.5 Materials for protein array

3.5.1 Accessories

Omnifix-F, 1 ml, Braun Melsungen Ltd. (Bad Arolsen, Germany)

Quantibody® Mouse TH17 Array 1, quantitative measurement of 18 mouse TH1-TH2-TH17 cytokines, RayBiotech Ltd. (Norcross, USA)

Sterican (size 14), 0,60x30 mm, Braun Melsungen Ltd. (Bad Arolsen, Germany)

3.6 Reagents for histological cuts

3.6.1 Chemicals

Alcian Blue solution, 1% in 3% acetic acid, ph 2,5, Sigma Aldrich Ltd. (Steinheim, Germany)

ddH_2O, produced in the lab with Arium®pro

Eosin Y disodium salt ≥85%, Sigma Aldrich Ltd. (Steinheim, Germany)

Ethanol ≥96%

Eukitt® Quick-hardening mounting medium for microscopy, Sigma Aldrich Ltd. (Steinheim, Germany)

Formalin solution, neutral buffered, 10% histological tissue fixative, Sigma Aldrich Ltd. (Steinheim, Germany)

Mayer's hematoxylin solution (Gill No.2), Sigma Aldrich Ltd. (Steinheim, Germany)

Paraffin Wax, Sigma Aldrich Ltd. (Steinheim, Germany)

Periodic acid ≥99,0%, Sigma Aldrich Ltd. (Steinheim, Germany)

Schiff's reagent for aldehydes for microscopy, Sigma Aldrich Ltd. (Steinheim, Germany)

Xylene, histological grade, Sigma Aldrich Ltd. (Steinheim, Germany)

3.6.2 Preparation of solutions

Eosin
Stock solution: 2.0 g in 40 ml ddH2O and 160 ml 95% EtOH
Working solution: add 200ml stock solution to 600ml of 80% EtOH

Periodic acid (1%)
0,5 g periodic acid and 50 ml ddH20

3.7 Reagents for western blot

3.7.1 Chemicals

2-β-Mercaptoethanol, Sigma Aldrich Ltd. (Steinheim, Germany)

Acetic acid, 100%, Carl Roth Ltd. (Karlsruhe, Germany)

Ammoniumperoxodisulfat (APS), ≥98%, Carl Roth Ltd. (Karlsruhe, Germany)

Anti-mouse IgG, HRP-linked Antibody (#7076), Cell Signaling Technology Ltd. (Danvers, USA)

Anti-rabbit IgG, HRP-linked Antibody (#7074), Cell Signaling Technology Ltd. (Danvers, USA)

B-Actin (13E5) Rabbit mAb (#4970), Cell Signaling Technology Ltd. (Danvers, USA)

Bovine Serum Albumin (BSA) fraction V, Hoffmann-La Roche Ltd. (Basel, Switzerland)

Bromphenol blue sodium salt, Carl Roth Ltd. (Karlsruhe, Germany)

DTT (D-Dithiothreitol solution), 1 M in H2O, Sigma Aldrich Ltd. (Steinheim, Germany)

Ethanol, 70%

Glycerol, ≥98%, waterfree, Carl Roth Ltd. (Karlsruhe, Germany)

Glycine, ≥99% blotting grade, Carl Roth Ltd. (Karlsruhe, Germany)

HCl (Hydrochloric acid), 25%, Carl Roth Ltd.. (Karlsruhe, Germany)

IkBα Antibody Rabbit (#9242), Cell Signaling Technology Ltd. (Danvers, USA)

Methanol ROTISOLV® HPLC Gradient Grade, Carl Roth Ltd. (Karlsruhe, Germany)

Nonfat dried milk powder PanReac Applichem Ltd. (Barcelona, Spain)

Phospho-IkBα (Ser32/36) (5A5) Mouse mAb (#9246), Cell Signaling Technology Ltd. (Danvers, USA)

Pierce Phosphatase Inhibitor, Mini Tablets, Thermo Scientific Ltd. (Rockford, USA)

PierceTM BCA Protein Assay Kit, Thermo Scientific Ltd. (Rockford, USA)

Ponceau S, Sigma Aldrich Ltd. (Steinheim, Germany)

Precision Plus ProteinTM Dual Color Standards, Bio Rad Ltd. (Carlsbad, USA)

Precision Plus ProteinTM Standards, Dual color, Bio Rad (Hercules, USA)

Protease inhibitor cocktail tablets, cOmplete Mini, EDTA-free, Roche Diagnostics Ltd. (Mannheim, Germany)

RIPA Lysis Buffer, 10x, EMD Millipore Corp. (Billerica MA, USA)

Rotiphorese® Acrylamide/Bis-solution 30 (29:1), Carl Roth Ltd. (Karlsruhe, Germany)

SDS (sodium laurylsulfat), ≥99%, Carl Roth Ltd.. (Karlsruhe, Germany)

SuperSignalTM West Dura Extended Duration Substrate, Thermo Scientific Ltd. (Rockford, USA)

TEMED (N, N, N', N'-Tetramethylenediamine), ≥99%, Carl Roth Ltd. (Karlsruhe, Germany)

Tris ≥99,3% buffer grade, Carl Roth Ltd.. (Karlsruhe, Germany)

Tween®20 (Polyethylene glycol sorbitan monolaurate), Sigma Aldrich Ltd. (Steinheim, Germany)

3.7.2 Preparation of solutions

10x electrophorese buffer
30,28 g Tris (base), 144,13 g Glycin and 10 g SDS were dissolved in 1000 ml ddH2O (ph between 8,5 and 8,7). (storage at room temperature)

1x electrophorese buffer (TBS)
100ml of 10x Elektrophoresis buffer was diluted with 900 ml ddH2O. (storage at room temperature)

4x SDS-loading buffer
5,217 ml 1,5 M Tris was set to ph 6,8. 2,5 g SDS, 12,5 ml Glycerol, 5 ml 2-β-Mercaptoethanol and 12,5 mg Bromphenolblue were added. The mixture was filled up with ddH2O up to 25 ml. Aliquots were wrapped in aluminum foil. (storage at -20°C)

APS (10%)
0,1 g APS was dissolved in 1 ml ddH2O, always freshly prepared.

Blocking solution with bovine serum albumin (BSA)
1,25 g BSA was dissolved in 50 ml TBST. Blocking solutions were always freshly prepared for each run.

Blocking solution with non-fat dry milk powder
2,5 g milk powder was dissolved in 50 ml TBST. Blocking solutions were always freshly prepared for each run.

Detecting solution
1 ml of 1:1 dilution of SuperSignal™ West Dura Extended Duration Substrate was always prepared fresh and before the use stored in a dark room.

DTT (100mM)
30,85 mg DTT was dissolved in 2 ml ddH2O on ice and aliquoted. (stored at -20°C)

6,05 g Tris (base) was dissolved in 90 ml ddH2O. Then the pH was set by 6,8 with HCl and filled up to 100 ml with ddH2O. (storage at 4°C)

Ponceau-solution
0,1 g Ponceau S was dissolved in 500 µl acetic acid and 50 ml ddH2O)

RIPA buffer mix
1ml RIPA Lysis Buffer (10x, EMD Millipore, Billerica MA, USA), 9ml ddH2O, 1 tablet Pierce Phosphatase Inhibitor and 1 tablet Protease inhibitor cocktail were mixed

SDS (10%)
10 g SDS was dissolved in 100 ml ddH2O and heatened up to 45°C for better solubility. (storage at room temperature)

Towbin Transferbuffer
20 ml Methanol was mixed with 80 ml 1x Elektrophoresis buffer. (Storage at room temperature)

Washingbuffer (TBST)
1 ml Tween was mixed with 999 ml 1x-Elektophoresebuffer. (Storage at room temperature)

Separating gel (amount for two gels)
4170 µl ddH2O, 2600 µl 1,5 M Tris, 3330 µl 30% Acryl/Bis, 100µl 10% SDS, 100 µl 10% APS, 6 µl TEMED, always freshly prepared

Collecting gel (amount for two gels)
1512,5 µl ddH2O, 625 µl 0,5M Tris, 312,5 µl 30% Acryl/Bis, 25 µl 10% SDS, 25 µl 10% APS, 3 µl TEMED, always freshly prepared

3.7.2.1 Primary antibody solutions

β-Actin - 3 µl β-Actin Rabbit mAb was mixed with 2997 µl BSA blocking solution (1:1000).

IkBα - 3 µl IkBα Antibody Rabbit was mixed with 2997 µl BSA blocking solution (1:1000).

Phospho-IkBα - 3 µl Phospho-IkBα Mouse mAb was mixed with 2997 µl milk powder blocking solution (1:1000).

3.7.2.2 Secondary antibody solutions

β-Actin - 1 µl Anti-rabbit IgG, HRP-linked Antibody was mixed with 2999 µl BSA blocking solution (1:3000).

IkBα - 1 µl Anti-rabbit IgG, HRP-linked Antibody was mixed with 2999 µl BSA blocking solution (1:3000).

Phospho-IkBα - 1 µl Anti-mouse IgG, HRP-linked Antibody was mixed with 2999 µl milk powder blocking solution (1:3000).

3.8 Reagents for qRT-PCR

3.8.1 Chemicals

PerfeCTa® SYBR® Green FastMix®, Quanta bio (Beverly, USA)

Table 1: Primer sequences for qRT-PCR analysis of markers in small intestine epithelium tissues

Gene		Sequence
ATG7	fw	5‘ GTTCGCCCCCTTTAATAGTGC 3‘
	rv	5‘ TGAACTCCAACGTCAAGCGG 3‘
ATG12	fw	5‘ TAGAGCGAACACGAACCATCC 3‘
	rv	5‘ CACTGCCAAAACACTCATAGAGA 3‘
Eef1a1	fw	5’ CCTGGCAAGCCCATGTGT 3’
	rv	5’ TCATGTCACGAACAGCAAAGC 3’
GSTA3	fw	5‘ GAATGGAGCCTATCCGGTGG 3‘
	rv	5‘ GCATGGCGGTACAAGCCTTT 3‘
MGST1	fw	5‘ CCTTCTCCCTGGATTCAGTCAT 3‘
	rv	5’ TCGGCCATGCTTCCAATCTT 3‘

forward (fw), reverse (rv), quantitative real-time polymerase chainreaction (qRT-PCR), autophagy-related protein 7 (ATG7), autophagy-related protein 12 (ATG12), eukaryotic translation elongation factor 1 α1 (Eef1a1), glutathione S-transferase3 (GSTA3), microsomal glutathione S-transferase 1 (MGST1)

Table 2: Primer sequences for qRT-PCR analysis of fecal bacteria

Gene		Sequence
Bacteroidetes	fw	5‘GTTTAATTCGATGATACGCGAG 3‘
	rv	5‘TTAASCCGACACCTCACGG 3‘
Deferribacter	fw	5‘CTATTTCCAGTTGCTAACGG 3‘
	rv	5‘GAGATGCTTCCCTCTGATTATG 3‘
Firmicutes	fw	5‘TGAAACGTGAAGGAATTGACG 3‘
	rv	5‘ACCATGCACCACCTGTC 3‘
Lactobacillus	fw	5‘AGCAGTAGGGAATCTTCCA 3‘
	rv	5‘ CACCGCTACACATGGAG 3‘
Streptococcus	fw	5’ GAAGAATTGCTTGAATTGGTTGAA 3’
	rv	5’ GGACGGTAGTTGTTGAAGAATGG 3’
Parasutterella	fw	5‘ AACGTGTCCGCTCGTGGGGAC 3‘
	rv	5’ CGGAATAGCTGGATCAGGCTTG 3’
16sRNA	fw	5‘ TCCTACGGGAGGCAGCAGT 3‘
	rv	5’ GGACTACCAGGGTATCTAATCCTGTT 3’

3.8.2 Preparation of solutions

Master mix (amount per reaction)

2,4 µl ddH2O, 5 µl SYBR® Green FastMix®, 0,3 µl primer forward and 0,3 µl primer reverse.

3.9 Reagents for protein array

3.9.1 Chemicals

Phenylmethylsulfonyl fluoride (PMSF), Sigma Aldrich Ltd. (Steinheim, Germany)

RIPA Lysis Buffer, 10x, EMD Millipore Corp. (Billerica MA, USA)

3.9.2 Preparation of solutions

1x wash buffer I:
30ml of 20x wash buffer I were diluted with 570 ml ddH2O

1x wash buffer II:
30ml of 20x wash buffer II were diluted with 570 ml ddH2O

4 Methods

4.1 Animals intervention experimental protocol

To verify if different fasting diets may have a beneficial impact on the inflammation in the gastrointestinal tract, 56 male C57BL/6NRj mice were divided into seven groups of eight mice receiving following diets: control diet (CTL), caloric restriction (CR), intermittent fasting (IF), fasting mimicking diet (FMD), ketogenic diet 1 (Keto-1), ketogenic diet 2 (Keto-2) and ketogenic control diet (Keto-CTL).

The CTL diet comprised of 58% carbohydrates, 33% protein and 9% fat and was fed *ad libitum*. For CR and IF the same diets were used as for the control, but with restricted amounts or time periods of feeding. The CR diet involved 25% daily calorie reduction compared to average voluntarily food intake. The amount of chow which ad libitum mice ate was measured and calculated preceding CR. The rodents were fed once a day at five p.m. The IF group ate food ad libitum every second day. On the other day they had to fast. The FMD diet comprised of alternating periods of fasting and standard chow in between. The FMD diet started with a fasting cycle of four days, followed by seven days food ad libitum. The first fasting day comprised a 50% calorie reduction of the energy intake, the second 90%. The supplements given on these four days were extra virgin olive oil, essential fatty acids, and a vegetable mix. In total, three fasting cycles were performed.

Mice fed the three ketogenic diets had free access to food. The Keto CTL diet comprised 57% carbohydrates, 16% proteins, and 7% long-chain triacylglycerol (LCT). The Keto-1 included 75% LCT, 1% carbohydrates, and 8% protein. Keto-2 diet contained 50% LCT and 25% middle-chain triacylglycerol (MCT) as fat sources. A characterization of the diet composition of each group is listed in the table below.

Table 3: Animal intervention experimental protocol

Groups	**Food composition and dietary regime**	**Time of intervention**
Control	58% carbohydrates, 33% protein and 9% fat *ad libitum*	5 weeks
CR	Control diet with 25% caloric reduction each day	2 weeks
IF	Control diet *ad libitum* every second day	2 weeks
FMD	Fasting day 1: 6% broth powder, 13% extra olive oil, 0,2% essential FA, 15% vegetable mix mixed in 66% hydrogel Fasting day 2-4: 5% broth powder, 1% glycerol in 94% hydrogel During fasting days, 7 days control diet *ad libitum*	3,5 weeks
Keto-1	8% protein, 75% LCT, 1% sugar, 10% crude fibre and 4% crude ash *ad libitum*	5 weeks
Keto-2	8% Protein, 50% LCT, 25% MCT (15% C8 and 10% C10), 1% sugar, 10% crude fibre and 4% crude ash *ad libitum*	5 weeks
Keto-CTL	16% protein, 7% LCT, 6% sugar, 51% starch, 10% crude fibre and 4% crude ash ad libitum	5 weeks

Control diet (CTL), caloric restriction (CR), intermittent fasting (IF), fasting mimicking diet (FMD), ketogenic diet 1 (Keto-1) and ketogenic diet 2 (Keto-2), ketogenic control diet (Keto-CTL), long-chain triacylglycerol (LCT), middle-chain triacylglycerol (MCT), caprylic acid (C8), capric acid (C10)

4.1.1 Tissue collection

After the food interventions, the mice were euthanized (isoflurane in oxygen), heart-punctured and dissected. All mice were killed at the same age. The tissue samples for the histological cuts were collected from the early ileum and colon. The tissue for histology was fixed in 4% buffered paraformaldehyde (PFA) directly after dissection. For protein and gene expression analysis small intestine epithelium tissues were collected and for bacteria quantification additionally the feces. Both were stored in -80°C till usage.

4.2 Histological stains: sample harvesting, cutting and staining

The tissue was fixed in 4% buffered paraformaldehyde (PFA) for 24h at 4 °C. After rinsing the samples in phosphate-buffered-saline (PBS) they were dehydrated in ethanol (EtOH) and incubated in xylene prior embedding in paraffin. The dehydration steps included the incubation of the tissue in 80% EtOH for 45 minutes, followed by an incubation in 95% EtOH mixed with 5% MeOH for 45 minutes. Afterwards the samples were incubated 3 times in 100% EtOH for 1 hour each, followed by the incubation in xylene 2 times for 45 min and 2 times in paraffin for 1 hour.

For the cutting step, the FFPE tissue blocks were cut into 4 µm sections using a microtome and affixed on a microscope glass. The glasses were dried in the incubator at 37°C for three days.

4.2.1 H&E stains experimental protocol for colon and small intestine

To examine histological differences between the diet groups hematoxylin and eosin staining (H&E) was performed. Before the tissue could be stained, it was dewaxed and dehydrated. For the dewaxing step xylene was used and for the dehydration step different concentrations of EtOH. Afterwards the tissue was rinsed in double distilled water (ddH20), stained in hematoxylin solution for two minutes, rinsed again in tap water and ddH20, dehydrated, counter stained in eosin for 2 seconds, dehydrated and cleaned with xylene before cover slipping. The exact steps of the protocol are shown in figure 4.

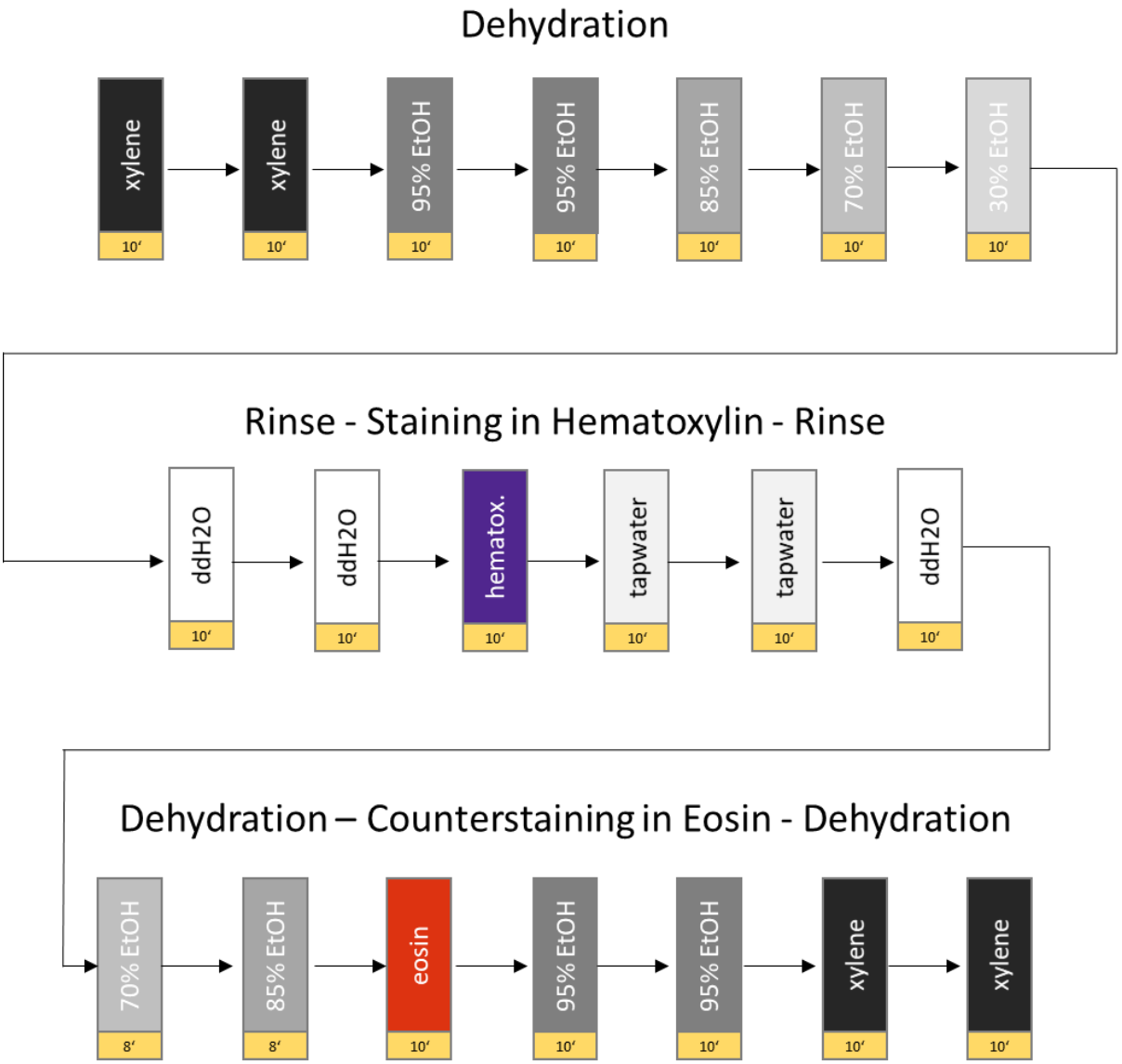

Figure 4: H&E staining protocol. Ethanol (EtOH), double distilled water (ddH20), hematoxylin (hematox.), 10 minutes (10’), 10 seconds (10s; The yellow rectangles show the incubation time of the solvents.

Microscopic pictures from the histological cuts were taken with a camera and a ZEN software. The thickness of the muscularis externa, the length of the villi intestinalis and the depth of the crypts were analyzed with the scale-bar tool from ImageJ software. The averages were calculated in excel. The statistical significance was verified using the t-test in consideration of the α error accumulation.

4.2.2 Goblet cell stains experimental protocol for colon

Goblet cell staining was performed to differentiate the goblet cells from the epithelial cells in the colon and observe the amount of this cell population. The staining components are alcian blue, periodic acid and Schiff's reagent.

For the staining step, the tissue was dewaxed in xylene and dehydrated in decreasing concentrations of EtOH. Afterwards the tissue was rinsed in ddH20 before alcian blue solution (1%) was pipetted directly on the samples. The microscopy glasses were incubated in a wet room for 30 minutes. Then the samples were rinsed in tap water for 3 minutes and 10 seconds in ddH20. Next, periodic acid (1%) was pipetted on the tissue, incubated for 10 minutes in the wet room and rinsed again in tap water for 3 minutes and ddH20 for 10 seconds. Afterwards, Schiff's reagent was pipetted on the tissue, incubated for 15 minutes, rinsed again in tap water and ddH20 as before. After that, the tissue was counter stained with hematoxylin for 2 minutes, followed by rinsing in tap water for 20 seconds and ddH20 for 10 seconds. The last steps were dehydrating the tissue in ascending concentrations in EtOH and cleaning it with xylene for 4 minutes before cover slipping. The steps of the protocol are shown in figure 5.

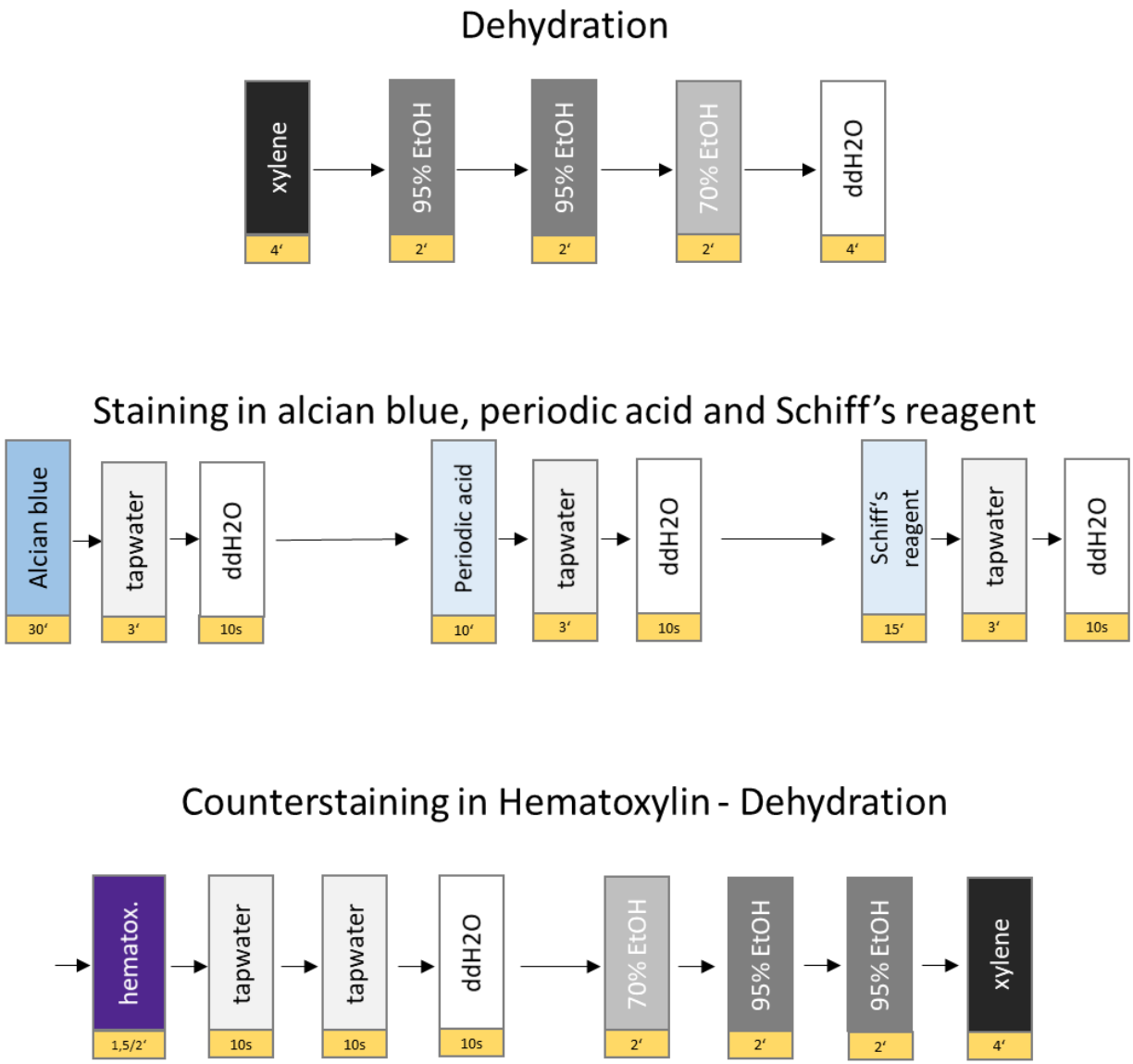

Figure 5: Goblet cell staining protocol

Microscopic pictures from the stained tissue were taken using the ZEN software.

4.3 Western blot experimental protocol

To further examine differences in the gastrointestinal tract, the concentration of IkBα was examined in the small intestine. As a reference β-Actin was used.

Western blot is an analytical technique to detect specific proteins in a solution. The proteins in the examined solution are separated using a gel electrophoreses. Afterwards the protein bands are blotted on a PVDF membrane, incubated with a primary and secondary antibody, and detected with a special analyzing system[88].

In this experiment small intestine epithelium tissue was lysed in RIPA buffer mixed with phosphatase and protease inhibitors. The extracted proteins were quantified using the PierceTM BCA protein determination method (Thermo Scientific, Rockford, USA).

For the gels, a separating and a collecting gel were produced. The composition of the gels is shown in the table below.

Table 4: Composition of the separating and collecting gel

SEPERATING GEL		**COLLECTING GEL**	
substances	**mass**	**substances**	**mass**
ddH2O	4170 µl	ddH2O	1512 µl
1,5M Tris	3330 µl	0,5M Tris	625 µl
30% Acryl/Bis	3330 µl	30% Acryl/Bis	312 µl
10% SDS	100 µl	10% SDS	25 µl
10% APS	100 µl	10% APS	25 µl
TEMED	6 µl	TEMED	3 µl

Acrylamide/bis-solution 30 (Acryl/Bis), ammoniumperoxodisulfat (APS), sodium laurylsulfat (SDS), N, N, N', N'-tetramethylenediamine (TEMED)

All the substances were mixed in the listed order. First, the separating gel was pipetted in the glass brackets, followed by 500 µl 70% EtOH to get rid of the bubbles. After 45 minutes the abundant EtOH was soaked up with a filter paper and the collecting gel was pipetted on the already polymerized separating gel. A 15 pocket comb was put straight up in the gel. After 30 minutes the space between the two glass brackets was filled up with cooled down (4°C) 1x concentrated electrophoresis buffer and the combs were removed.

The protein concentration was 1 µg/µl for β-Actin and 3 µg/µl for IkBα. 2,5 µl loading buffer were added to each sample and the difference to 10 µl was filled up with RIPA-buffer. 1,5 µl DTT was added to each sample on the thermomixer and the whole solution was incubated at 300 RPM, at 95°C for five minutes. Then the samples were directly placed again on ice. 2 µl of Precision Plus ProteinTM Standard was pipetted in the first pocket on the gel, followed by 10 µl of each sample mix in the following pockets. After pipetting the sample mixes, the container with the gels was filled up with cooled down (4°C) 1x electrophoresis buffer. The gel electrophoresis was run in the cold room (4°C) at 80 Volt for 10 minutes and then 2 hours at 90 Volt.

After the gel electrophoresis, the gels were removed carefully from the glass brackets and incubated in towbin transfer buffer gently shaking for 10 minutes. In the meantime, the membranes were activated in methanol for 20 seconds and soaked in towbin transfer buffer on the shaker. The filters were also shortly immersed in towbin buffer before placing them together with the membrane, the gel and another filter on the top in the cassette of the Trans-Blot® Turbo Transfer System. With a roller the bubbles were pressed out. The protein bonds were electro-blotted onto PVDF membranes using the Trans-Blot® Turbo Transfer System. The membranes dried then for one hour.

Subsequently, the successful transfer was verified with the ponceau solution. For that step, the membranes were reactivated in methanol for 20 seconds and incubated in ponceau solution by gentle shaking for 3 minutes. Afterward the membranes were washed in ddH20 and incubated in the blocking solutions on the shaker for one hour. The composition of the blocking- and primary antibody solution is shown in table 5.

Table 5: Composition of primary antibody solution

prim. antibody	blocking solution	dilution
β-Actin	TBST, 2.5% BSA	1:1000
IkBα	TBST, 5% BSA	1:1000

Bovine serum albumin (BSA), milk powder (MP), NF-ϰ-B inhibitor α (IkBα), 0.1% Tween-20 in 1x TBS (TBST), *1x electrophorese buffer (TBS).*

Protein bands were detected on the membrane using Phospho-IkBα primary antibody, IkBα primary antibody and β-Actin primary antibody as a reference. β-Actin and IkBα were incubated in BSA blocking solution and Phospho-IkBα in the milk powder blocking solution.

After incubating in the blocking solution for one hour, the membranes were placed in the respective antibody solutions and incubated over night by 4°C. On the next day, the membranes were washed in TBST for 5, 10 and 15 minutes gently shaking before they were placed in the secondary antibody solution. The composition of the secondary antibody solution is shown in the table below.

Table 6: Composition of secondary antibody solution

protein	sec. antibody	blocking solution	dilution
β-Actin	anti-rabbit IgG AB	TBST, 2.5% BSA	1:3000
IkBα	anti-rabbit IgG AB	TBST, 5% BSA	1:3000

Antibody (AB), bovine serum albumin (BSA), milk powder (MP), NF-ϰ-B inhibitor α (IkBα), 0.1% Tween-20 in 1x TBS (TBST), 1x electrophorese buffer (TBS), immunoglobulin G (IgG).

After one hour of incubation in the secondary antibody, the membranes were washed again in TBST for 5, 10 and 15 minutes.

For detection, the membranes were placed in the ChemiDoc XRS+ system. Before starting the machine, 1 ml of the detection solution was pipetted on the membrane. Quantitative analysis of the photographed bands was carried out using ImageJ software. Density of all three proteins were quantified and normalized. Then IkBα and Phospho- IkBα protein bands were put in proportion with β-Actin values.

4.4 qRT-PCR experimental protocol

The qRT-PCR was used to examine differences in the messenger ribonucleic acid (mRNA) gene expression of the autophagy-related proteins 7 and 12 (ATG7 and ATG12), microsomal glutathione S-transferase 3 (MGST1) and glutathione S-transferase 3 (GSTA3) in the small intestine epithelium tissue and the DNA level of *Lactobacillus, Deferribacter, Bacteroidetes, Firmicutes, Streptococcus* and *Parasutterella* in the feces. The fecal DNA was isolated using the innuPREP Stool DNA kit (Analytik Jena) according to the manufacturer's instructions.

The primers used for the qRT-PCR are listed in chapter 4.8.1. 2 µl of the DNA solution and 8 µl of the respectively master mix were pipetted on the 384-well PCR plate. The composition of the used master mixes is listed in the table below.

Table 7: Composition of the master mixes for qRT-PCR

substance	**amount per sample**
SYBR Green SuperMix	5 µl
ddH2O	2,4 µl
Primer forward from the respective primer	0,3 µl
Primer reverse from the respective primer	0,3 µl

Quantitative real-time polymerase chain reaction (qRT-PCR)

All PCR reactions were performed in triplicates. The program of the PCR thermocycler is listed in table below.

Table 8: Cycling conditions for qRT-PCR in the thermocycler

Genes	**Initial denaturation**	**Denaturation**	**Annealing, elongation**	**Melting curve**	**Cycles**
ATG7, ATG12, GSTA3, MGST1, Eef1a1, Deferribacter	95 °C, 20 s	95 °C, 1 s	60 °C, 20 s	95 °C, 15 s 60 °C, 60 s 95 °C, 15 s	40
Lactobacillus, Firmicutes, Bacteroidetes, Parasutterella, Streptococcus 16sRNA	95 °C, 20 s	95 °C, 1 s	62 °C, 20 s	95 °C, 15 s 62 °C, 60 s 95 °C, 15 s	40

Quantitative real-time polymerase chain reaction (qRT-PCR), autophagy-related protein 7 (ATG7), autophagy-related protein 12 (ATG12), eukaryotic translation elongation factor 1 α 1 (Eef1a1), glutathione S-transferase 3 (GSTA3), microsomal glutathione S-transferase 3 (MGST3)

The expression of the target genes was normalized to the stably expressed reference genes Eef1a1 and 16sRNA. The relative gene expression was calculated with the Δ-Δ-C_T-method using excel.

4.5 Protein array experimental protocol

Protein arrays enable determining multiple cytokine concentrations at the same time. It is a combination of the high detection sensitivity and specificity of enzyme-linked immunosorbent assays (ELISAs) and the high throughput of arrays. The method is based on two cytokine-specific antibodies for detection, a capture antibody that binds to the glass surface and a secondary antibody that binds on the specific cytokine. During the incubation with the sample, the target cytokines are trapped on the antibodies on the glass surface on which the secondary biotin-labeled antibody binds afterwards. The cytokine-antibody-biotin complex can be visualized by adding a streptavidin-conjugated equivalent dye with a laser scanner. Streptavidin binds to biotin with a high affinity [97, 103].

A standard glass slide comprises 16 wells with 18 identical cytokine antibodies bound to the glass surface. The two positive controls (POS1 and POS2) and each antibody are arrayed in quadruplicates. The figure below depicts the steps explained above.

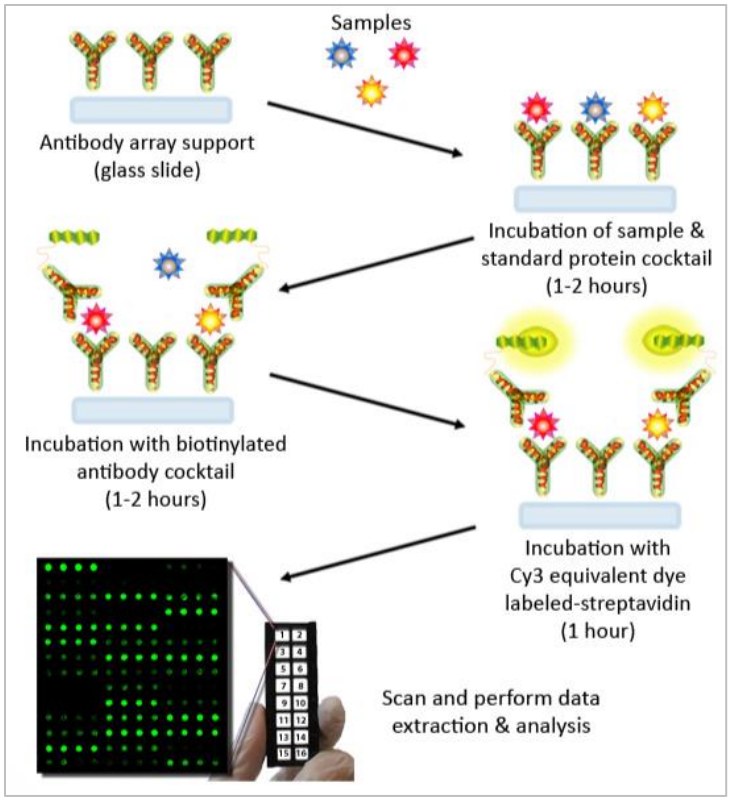

Figure 6: Flowchart of the protein array [103]

For the sample preparation, 10 mg of frozen small intestine epithelium tissue was cut and dissolved in 100 µl 1x RIPA-mix with PMSF on ice. Then the samples were centrifuged for 20 minutes, at 10 000 g, at 4°C. The pellet was left behind and the liquid part was transferred to a new tube. The sample concentration was measured photometrically according to the manual of the PierceTM BCA Protein Assay Kit (Thermo Scientific). For the protein array, a concentration of 1 µg/µl was used. The samples were stored at -80°C.

First, the cytokine standard dilutions were prepared. In the first vial, 500 µl of the Quantibody® sample diluent was pipetted. 200 µl water was added to the vials two to seven. Then 100 µl

were added of Std1 to tube Std2 and mixed gently. Five more serial dilutions were performed by adding 100 µl of Std2 to tube Std3 and so on. 100 µl sample diluent was pipetted in an empty tube for the negative control (CNTRL). The pipette scheme explained above is shown in figure 7.

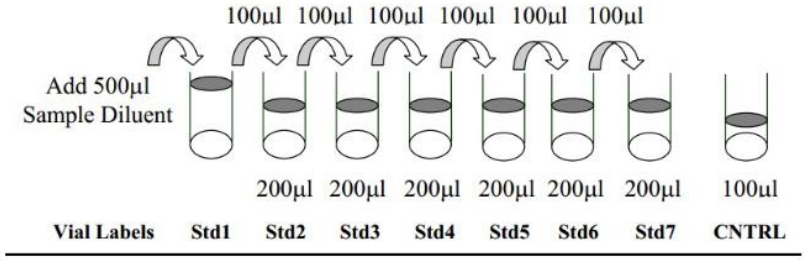

Figure 7: Pipetting scheme of the standards and the negative control.Standard 1 to 7 (Std 1-7), negative control (CNTRL)

100 µl sample diluent was pipetted into each well and incubated for 30 minutes to block the slides. After removing the diluent, 100 µl of sample or standards were pipetted in each well. Because of a limitation of 32 wells (two glass plates), two to three samples were merged and pipetted as one replicate on the protein array. The layout of the pipetted samples on the slides is shown in table 9.

Table 9: Layout of the samples on the Mouse Th12 array

Glass 1	
Std1	IF1
Std2	IF2
Std3	IF3
Std4	FMD1
Std6	FMD2
Std7	FMD3
CNTRL	Keto-11
Keto-13	Keto-12

Glass 2	
CTL1	Keto-21
CTL2	Keto-22
CTL3	Keto-23
CTL4	Keto-CTL1
CR1	Keto-CTL2
CR2	Keto-CTL3
CR3	CNTRL
CR4	Std4

Standard 1 to 7 (Std 1-7), negative control (CNTRL), intermittent fasting sample 1 (IF1), intermittent fasting sample 2 (IF2), intermittent fasting sample 3 (IF3), ketogenic diet 1 sample 1 (Keto-11), ketogenic diet 1 sample 2 (Keto-12), ketogenic diet 1 sample 3 (Keto-13), control diet sample 1 (CTL1), control diet sample 2 (CTL2), control diet sample 3 (CTL3), control diet sample 4 (CTL4), caloric restriction sample 1 (CR1), caloric restriction sample 2 (CR2), caloric restriction sample 3 (CR3), caloric restriction sample 4 (CR4), ketogenic diet 2 sample 1 (Keto-21), ketogenic diet 2 sample 2 (Keto-22), ketogenic diet 2 sample 3 (Keto-23), ketogenic control diet sample 1 (Keto-CTL1), ketogenic control diet sample 2 (Keto-CTL2), ketogenic control diet sample 3 (Keto-CTL3)

After incubation, the glasses were washed by decanting the solutions from each well and washing the wells 5 times for 5 minutes each with 150 µl 1x wash buffer I gently shaking. After decanting 1x wash buffer I from each well, the glasses were washed two times for five minutes each with 150 µl of 1x Wash Buffer II gently shaking.
To reconstitute the detection antibody, 1,4 ml of sample diluent was added to the Mouse TH17 Array 1 Biotinylated Antibody Cocktail tube. 80 µl of this detection antibody cocktail was pipetted in each well. After incubation, the solutions were decanted and washed five times for five minutes each with 150 µl of 1x wash buffer I and the 2 times with 150 µl of 1x wash buffer II gently shaking. Then the wash buffer was completely removed.
For the incubation with Cy equivalent dye-streptavidin, 1,4 ml of sample diluent was pipetted into the Cy3 equivalent dye-conjugated streptavidin tube. 80 µl of the mixture was added to each well and covered with aluminum foil. After one hour of incubating in the dark room, the samples were decanted, and the wells were washed five times for five minutes each with 150 µl of 1x wash buffer I gently shaking. After removing the wash buffer, the clips were disassembled by pushing the clips outward from the slide.
The two glasses were carefully placed in the slide washer/dryer (a slide holder centrifuge tube). 30 ml of 1x wash buffer I was added to the tube to cover the whole slides. After gently shaking for 15 minutes the buffer was decanted and the same procedure was made with 1x wash buffer II for 5 minutes.

The glasses were sent for fluorescence detection using a laser scanner. The results data sent back was analyzed using excel. Statistically significant differences between the averages of the groups were calculated with the t-test in consideration of the α error accumulation.

5 Results

5.1. H&E staining in the small intestine and colon

To visualize the impact of different diets on the intestinal morphology, H&E staining was performed. The staining was used for quantification of the length of villi intestinalis, the depth of crypts and the thickness of muscularis externa. The photomicrograph below shows how the measurement was executed.

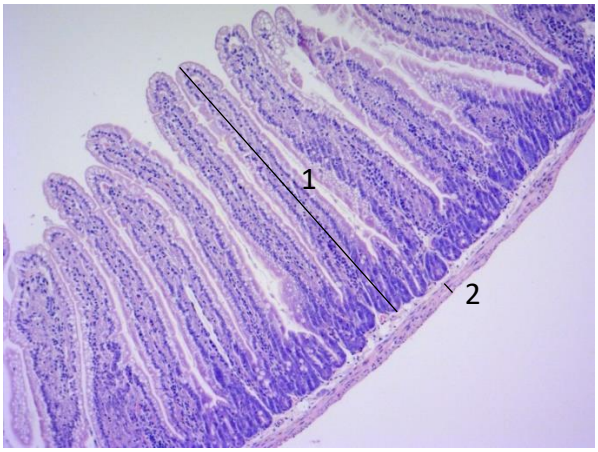

Figure 8: Measurement of the length of villi intestinalis (1) and thickness of muscularis externa (2) in intestinal tissue samples. Magnification, 100

5.1.1 Results of H&E staining in the colon

Regarding the crypt depth in the colon, the Keto-2 mice showed a decrease in the depth compared to all other groups. The crypt depth was statistically significantly reduced in this group compared to the Keto-1, FMD and IF *($p < 0,0071$)* groups. The difference between the Keto-2 mice and the Keto-CTL *($p = 0,016$)* and CTL mice *($p=0,022$)* showed a strong trend of a decrease.

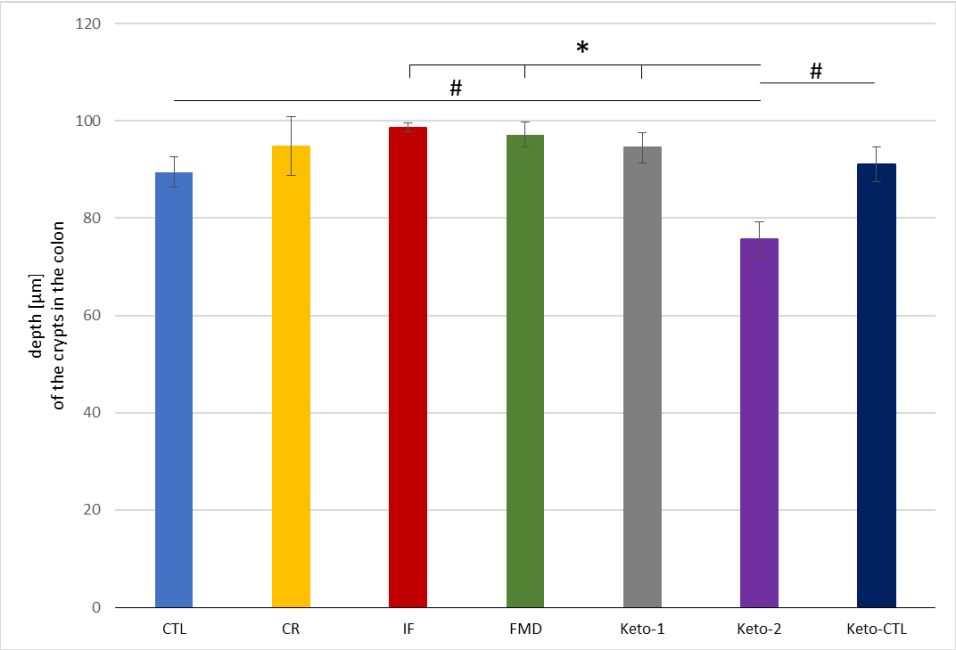

Figure 9: depth of crypts in the colon. # depicts strong trends (p=0,0071 to p=0,05), asterisk (*) depicts statistically significant differences (p>0,0071).

The photomicrographs below show excerpts of the crypts in the colon.

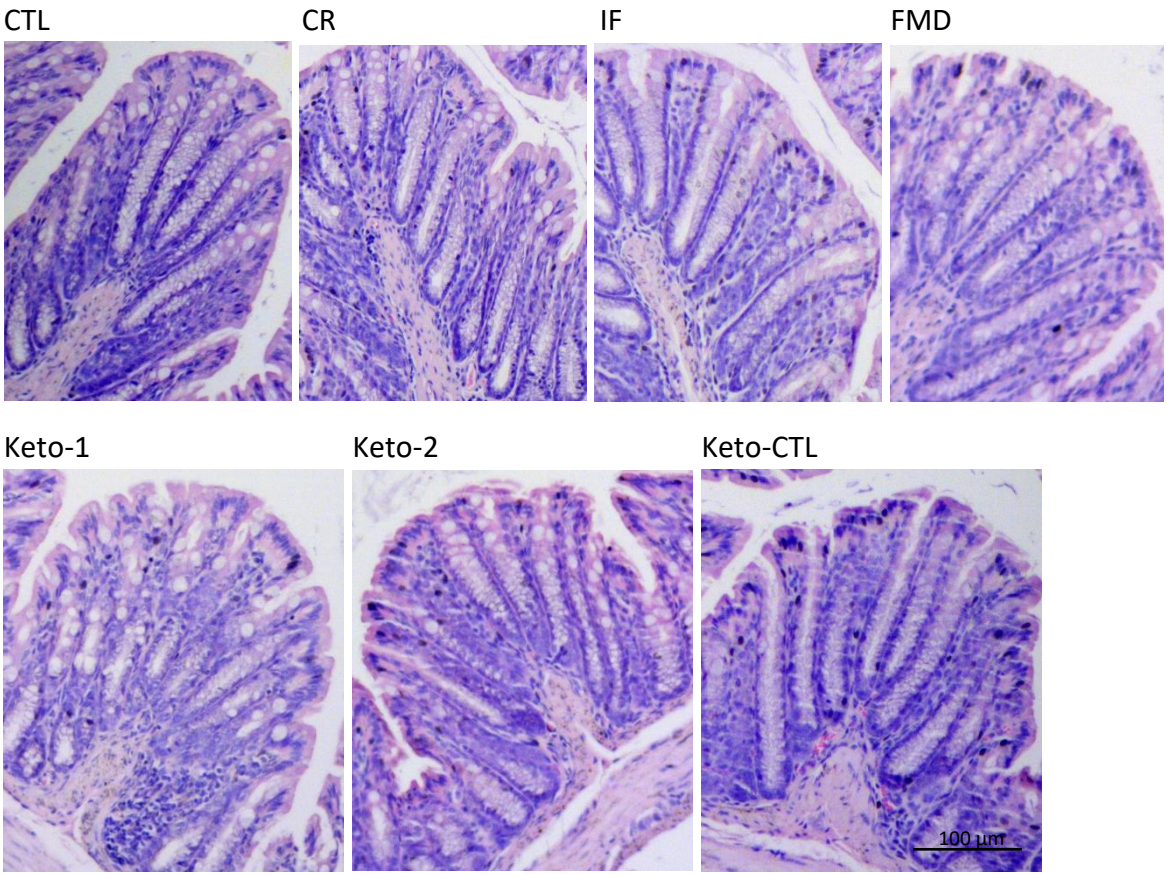

Figure 10: Photomicrographs of crypts in the colon. Magnification, 100

The figure below shows the results of measuring the thickness of the muscularis externa in the colon. Some values in the CTL group were higher, but no significant differences could be measured.

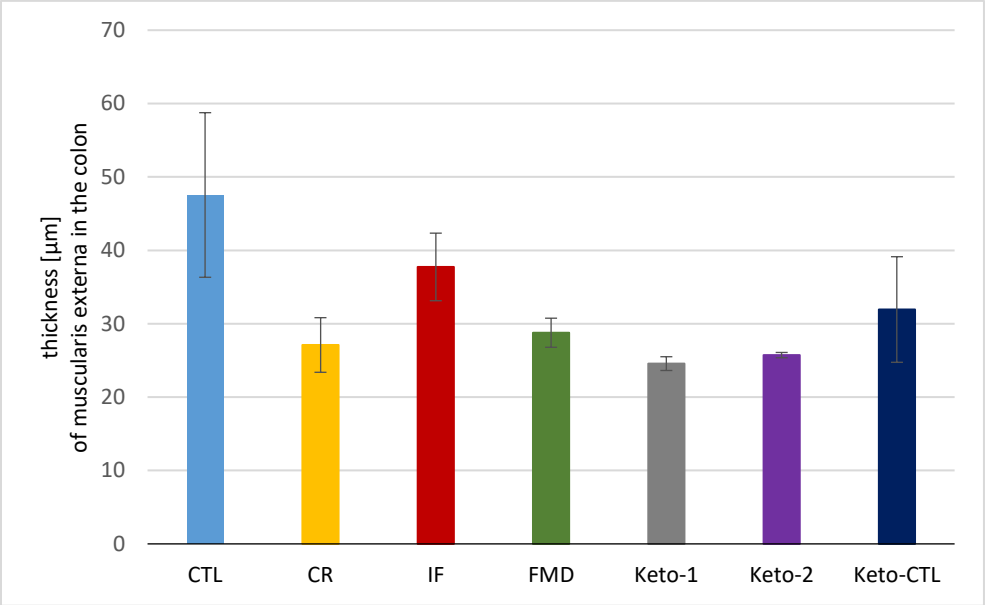

Figure 11: Thickness of muscularis externa in colon

Figure 12 shows the colon cross-sections in all diet groups. A tendency of a thicker muscularis externa in the CTL group was visible.

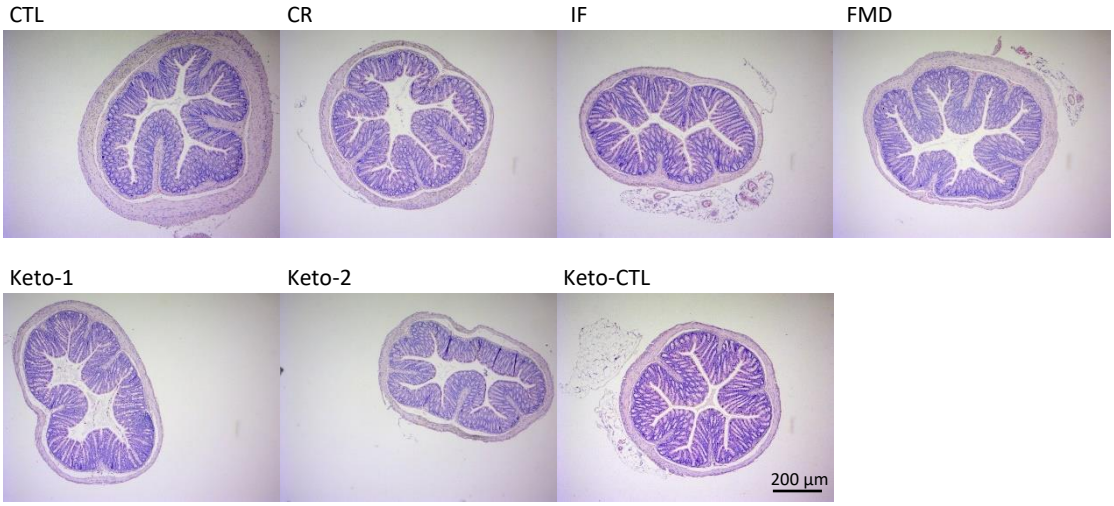

Figure 12: Photomicrographs of colon cross-sections. Magnification, 50

5.1.2 Results of H&E staining in the small intestine

Regarding the length of the villi intestinalis in the small intestine, the Keto-1 and Keto-2 mice had the longest villi compared to all other groups. A strong trend was measured for the increase of the Keto-1 and Keto-2 groups compared to the FMD group *(p=0,038 and p=0,041)* and the CR group compared to the IF *(p=0,035)* and Keto-CTL groups *(p=0,039).*

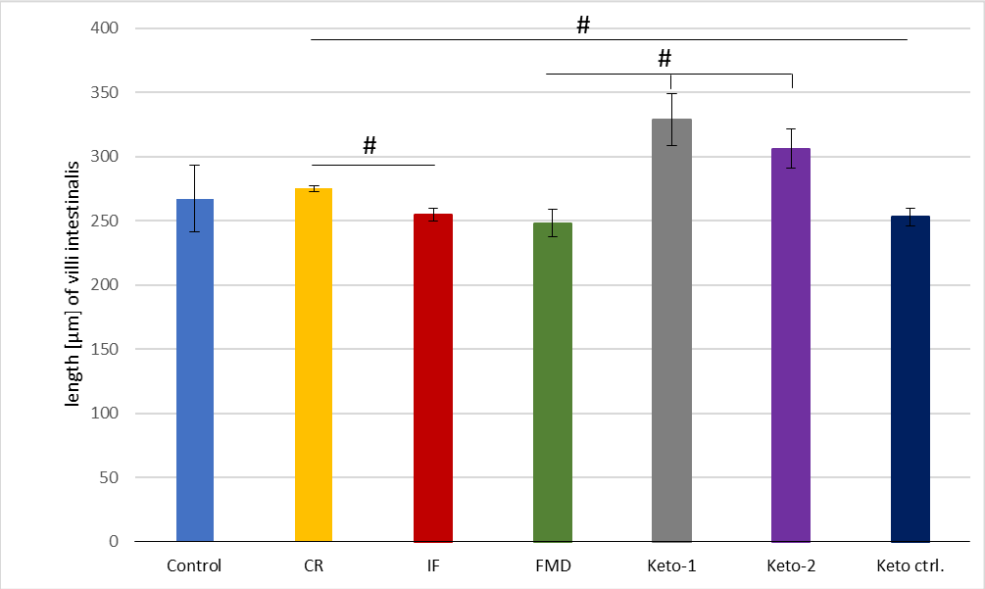

Figure 13: Length of villi intestinalis in early ileum

Regarding the thickness of muscularis externa in the small intestine, the ketogenic diets showed the thinnest muscle cross-sections. The thickness of muscularis externa in the Keto-1, Keto-2 and Keto-CTL mice was statistically significantly lower compared to the FMD mice *(p < 0,0071).* The difference between the IF mice and the FMD *(p=0,010),* Keto-1 (p=0,022) and Keto-2 mice *(p=0,018)* was almost statistically significant. The IF *(p=0,045),* Keto-1 *(p=0,014),* Keto-2 *(p=0,018)* and Keto-CTL mice *(p=0,023)* showed a strong trend for a reduction of the thickness of the muscularis externa.

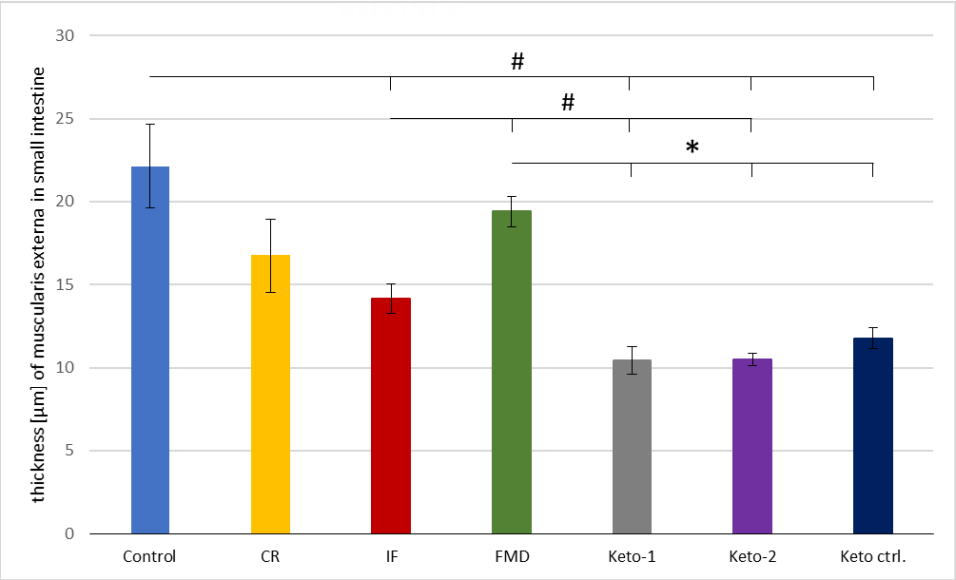

Figure 14: Thickness of muscularis externa in ileum. Asterisks depict the statistically significant difference p<0,0071.

Photomicrographs of small intestinal cross-sections are shown in the figure below. Clearly visible is that the CTL-mice had the thickest muscularis externa. Contrary, the Keto-1, Keto-2, Keto-CTL and IF mice had the thinnest one.

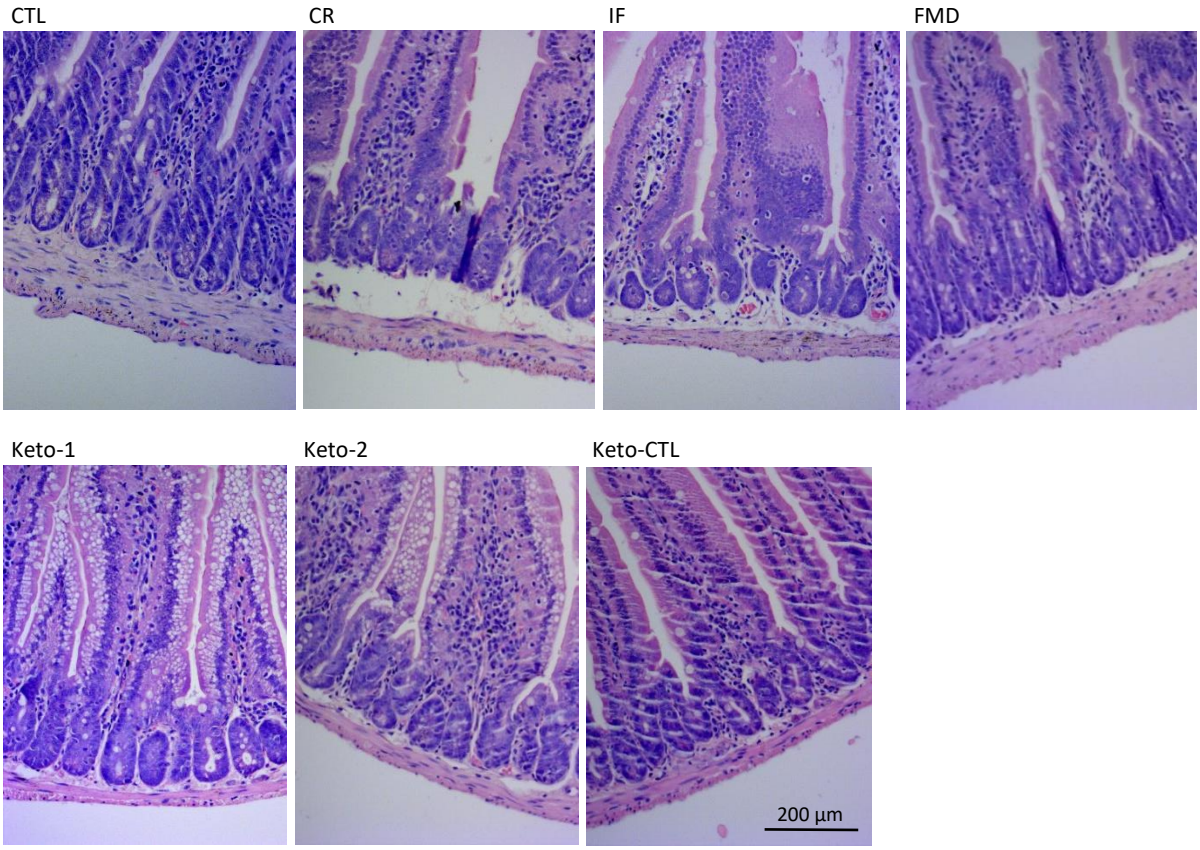

Figure 15: Photomicrographs of the muscularis externa in early ileum. Magnification, 200

These data from the H&E staining show that the intestinal morphology was statistically significantly altered in mice fed with different diets.

5.2 Goblet cell staining in the colon

To visualize the number of goblet cells in the colon, goblet cell staining was performed. A look at the images in figure 16 shows, that Keto-1 mice tended to have a lower number of goblet cells in the colonic mucosa compared to the other diets. No strong differences, however, were seen between the rest of the restrictive diet groups.

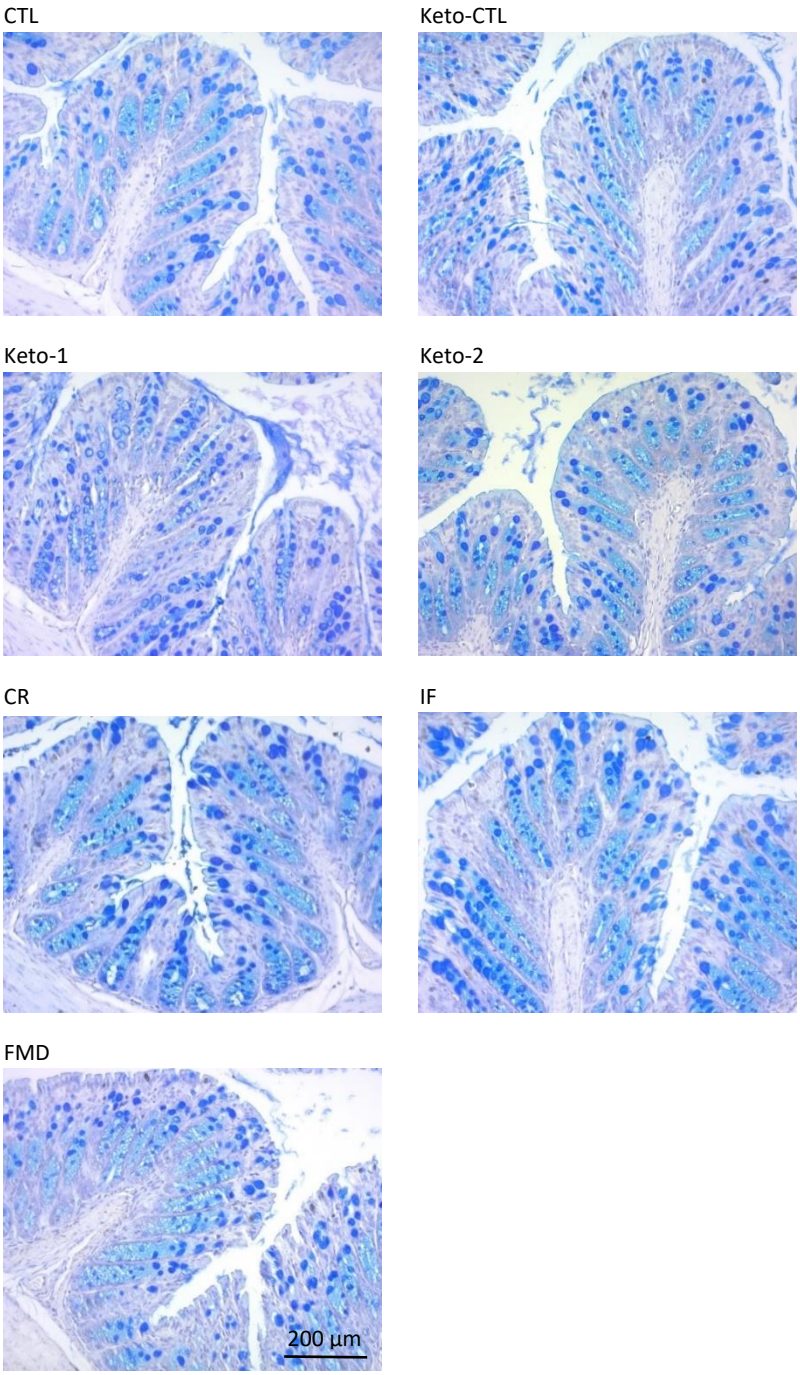

Figure 16: Photomicrographs of the goblet cells in the crypts in the colon. Magnification, 200

5.3 Western Blots in the small intestine epithelium tissue

To examine the expression of IkBα in the small intestine epithelium tissue, western blots were performed. The IF group had the highest IkBα concentration and the CTL group in contrast the lowest. The elevated IkBα levels from IF *(p=0,035),* Keto-1 *(p=0,016)* and Keto-2 groups *(p=0,021)* showed a strong trend of increase compared to the CTL mice as well as the increased expression in the FMD group compared to the Keto-1 group *(p=0,033).*

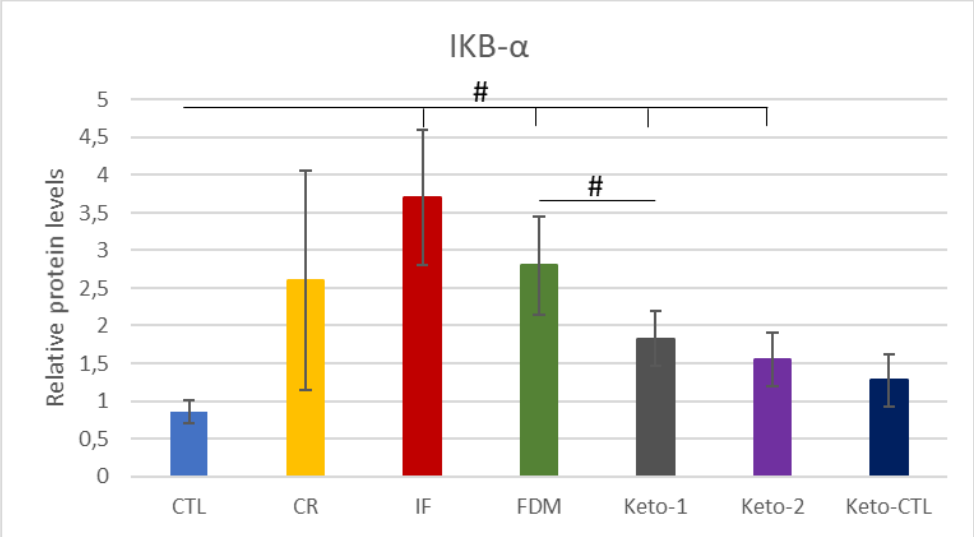

Figure 17: Relative protein levels of IkBα

The protein expression from Actin and IkBα is shown in figure 18. Actin was used as the reference protein.

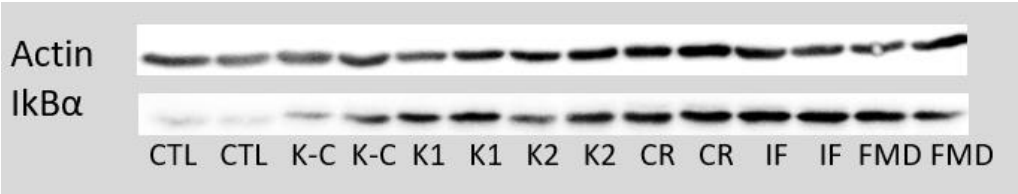

Figure 18: Actin and IkBα expression

5.4 qRT-PCR analysis in the small intestine epithelium tissue

The mRNA expression of GSTA3, MGST1, ATG7 and ATG12 in the small intestine epithelium tissue was measured via qRT-PCR. The results of the relative gene expression are shown in the figures below.

5.4.1 mRNA expression of GSTA3 in the small intestine epithelium tissue

Some values of the mRNA expression of GSTA3 in the Keto-1 mice were higher compared to all other groups, but no significances could be measured. A statistically significant increase was measured between the FMD and CTL group *(p < 0,0071).* A strong trend was measured between the Keto-2 (*p = 0,013)* and CR mice (*p = 0,016)* compared to the CTL mice.

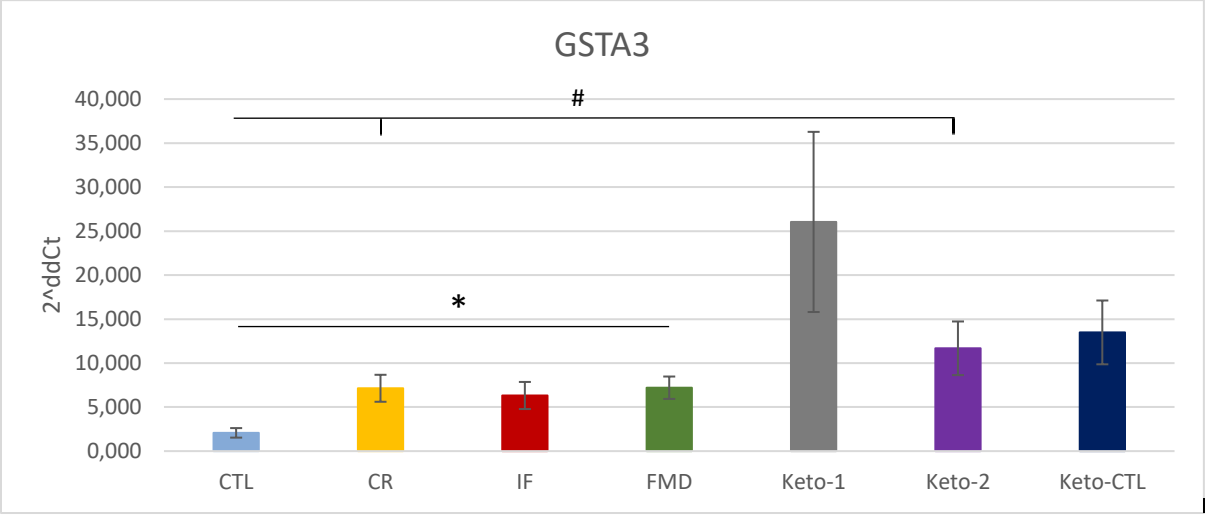

Figure 19: GSTA3 gene expression in small intestine epithelium tissue. Glutathione S-transferase 3 (GSTA3).

5.4.2 mRNA expression of MGST1 in the small intestine epithelium tissue

As shown in figure 20, the Keto-1 mice had the highest expression of MGST1, followed by the Keto-CTL and IF mice. Contrary, the CTL mice had the lowest mRNA expression. Statistically significant differences were measured between the CTL mice compared to the IF, FMD, Keto-1 and Keto-2 mice *(p < 0,0071)* and between the CR mice compared to IF, FMD and Keto-1 mice *(p < 0,0071).* Although some values were higher in the Keto-1 group compared to the Keto-2 group, no significant differences were measured between these two groups.

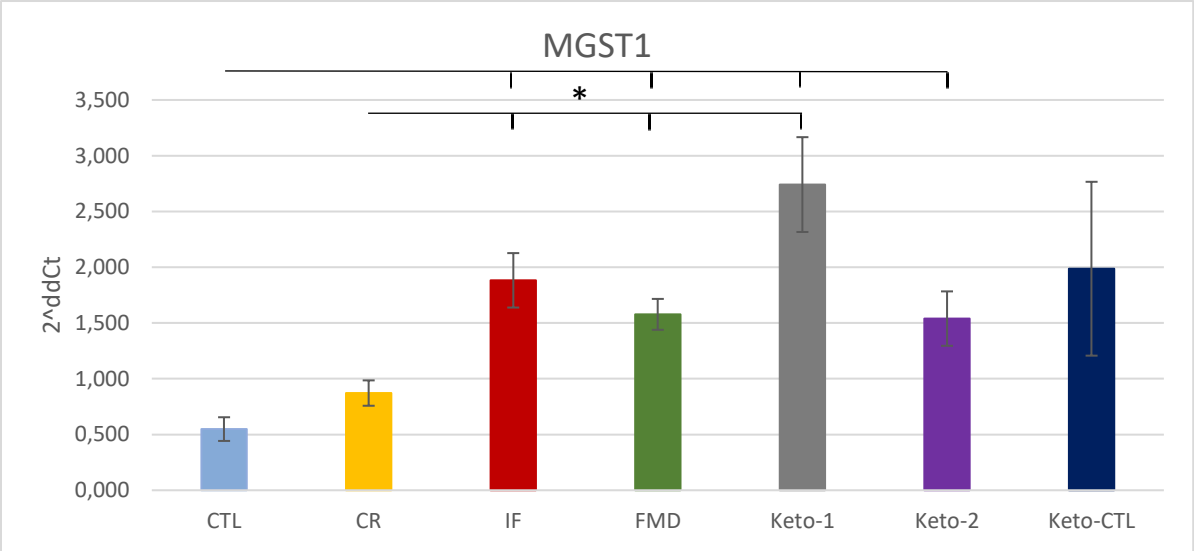

Figure 20: MGST1 gene expression in small intestine epithelium tissue. Microsomal glutathione S-transferase 1 (MGST1).

5.4.3 mRNA expression of ATG7 and ATG12 in the small intestine epithelium tissue

Regarding the mRNA expression of ATG7 in the small intestine epithelium tissue, the FMD mice had the highest gene expression, ATG12 was most strongly expressed in the Keto-1 group. However, no statistically significant differences were measured in both gene expressions.

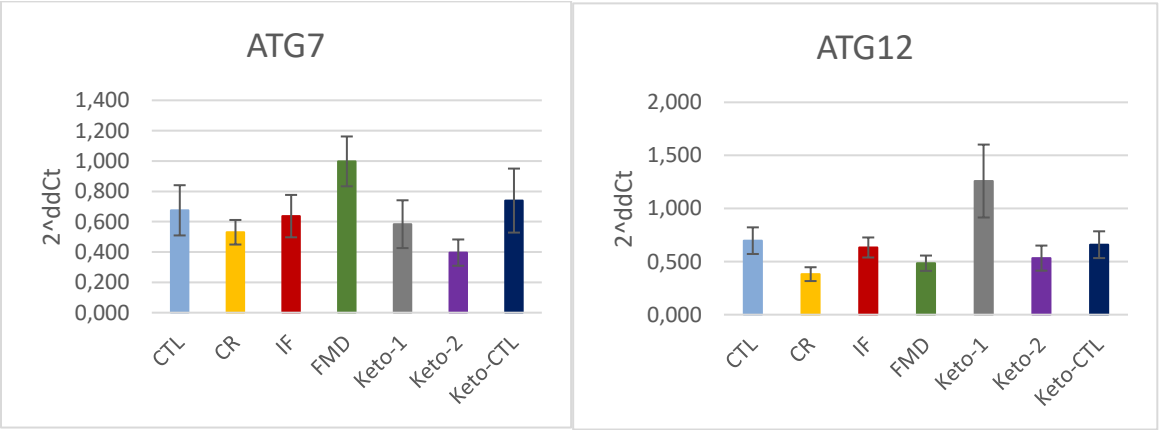

Figure 21: ATG7 and ATG12 gene expression in small intestine epithelium tissue. Autophagy-related 7 gene (ATG7), autophagy-related gene 12 (ATG12).

5.5 qRT-PCR analysis of fecal bacteria

To determine the DNA abundance of several bacteria in the different diet groups, qRT-PCRs from feces samples were performed. The following figures show the DNA abundance of *Parasutterella, Deferribacter, Bacteroidetes, Lactobacillus, Firmicutes* and *Streptococcus*.

5.5.1 DNA analysis of *Parasutterella* in the feces

This experiment showed a decrease of the *Parasutterella* abundance by ketogenic diets, especially by the Keto-2 and Keto-CTL diets. The reduction of the Keto-2 and Keto-CTL mice compared to CR mice was statistically significant *(p < 0,0071)*. A strong trend between the Keto-2 and Keto-CTL mice compared to CTL *(p = 0,015) and* IF mice *(p = 0,008)* was measured. The increase of the CR mice compared to Keto-1 mice was almost statistically significant *(p = 0,013)* as well as the difference between the higher expressed levels in the IF mice compared to Keto-2 and Keto-CTL mice. Some values in the FMD group were higher, but nonetheless, no significant differences were measured.

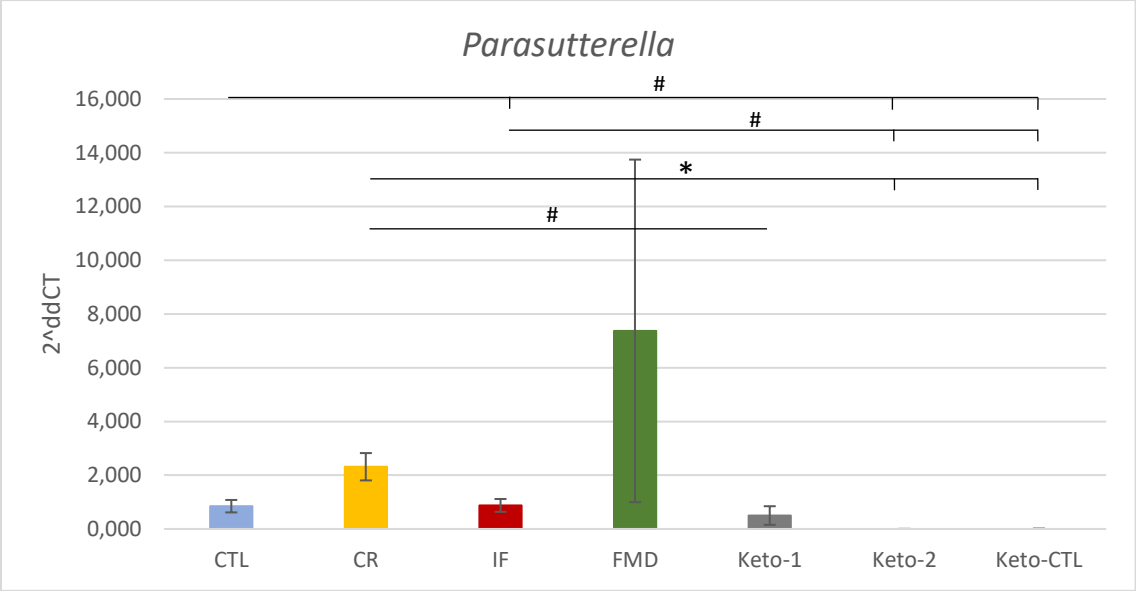

Figure 22: Gene analysis of Parasutterella in small intestine epithelium tissue

5.5.2 DNA analysis of *Deferribacter* in the feces

The gene analysis of *Deferribacter* showed the greatest differences from all bacteria. The Keto-1 and Keto-2 mice had the highest numbers of these bacteria. But because of the high deviations in these groups, statistically significant differences were only measured between the Keto-CTL group compared to the CR, IF and FMD groups *(p ≤ 0,0071).*

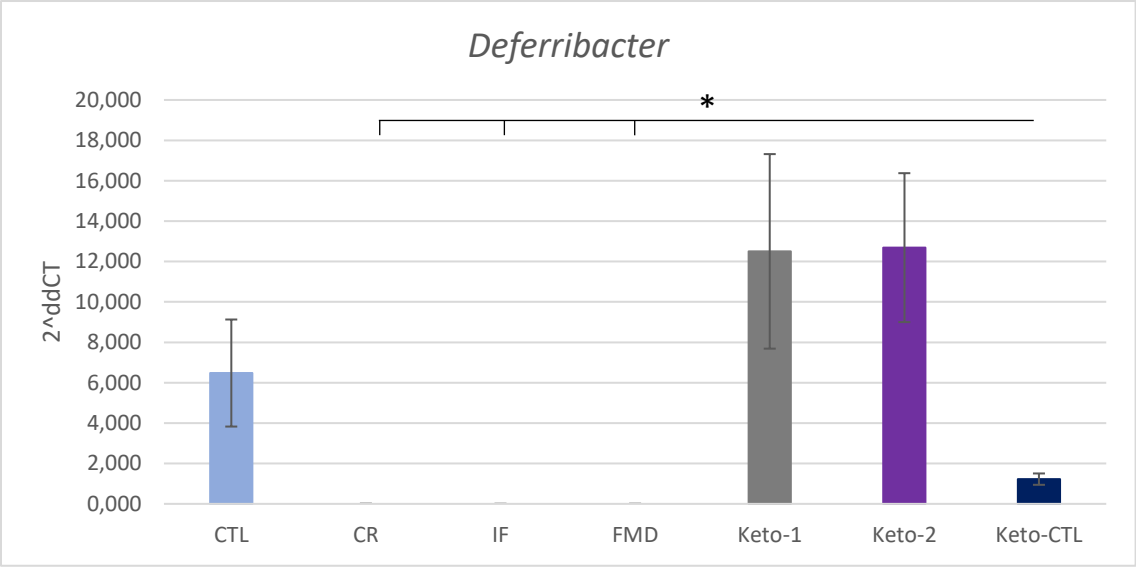

Figure 23: Gene analysis of Deferribacter in small intestine epithelium tissue

5.5.3 DNA analysis of *Bacteroidetes* in the feces

The three Keto diets showed lower levels of *Bacteroidetes* compared to the other groups. Statistically significant differences were measured between the Keto-CTL and CR mice *($p \leq 0{,}0071$),* strong trends were measured between the Keto-CTL and FMD mice *($p = 0{,}011$)* as well as between the Keto-2 and CR mice *($p = 0{,}014$).*

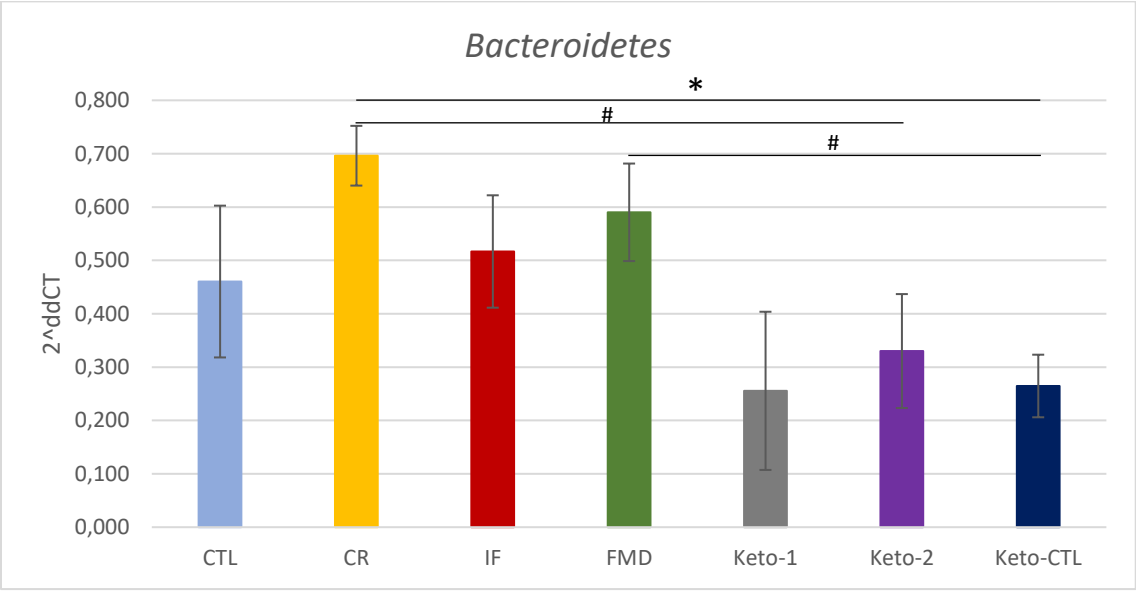

Figure 24: Gene analysis of Bacteroidetes in small intestine epithelium tissue.

5.5.4 DNA analysis of *Lactobacillus* in the feces

The CR and IF mice showed the highest amounts of *Lactobacillus* in the feces. The difference between these two groups compared to the lowest expressed groups, namely the Keto-1 and Keto-2 groups, was statistically significant *(p ≤ 0,0071)* as well as the difference between the CR diet compared to the FMD and CTL diets *(p ≤ 0,0071)*. Moreover, the IF mice showed a strong trend of an increased level of Lactobacillus in the feces compared to the CTL *(p=0,024),* FMD *(p=0,021)* and Keto-CTL mice *(p=0,040)* as well as the CR mice compared to Keto-CTL mice *(p=0,010).* A strong trend of a decrease was also measured in the Keto-1 *(p=0,042)* and Keto-2 groups *(p=0,010)* compared to the FMD group. The difference of the bacteria number between these two ketogenic diets compared to the CTL group was significant *(p ≤ 0,0071).*

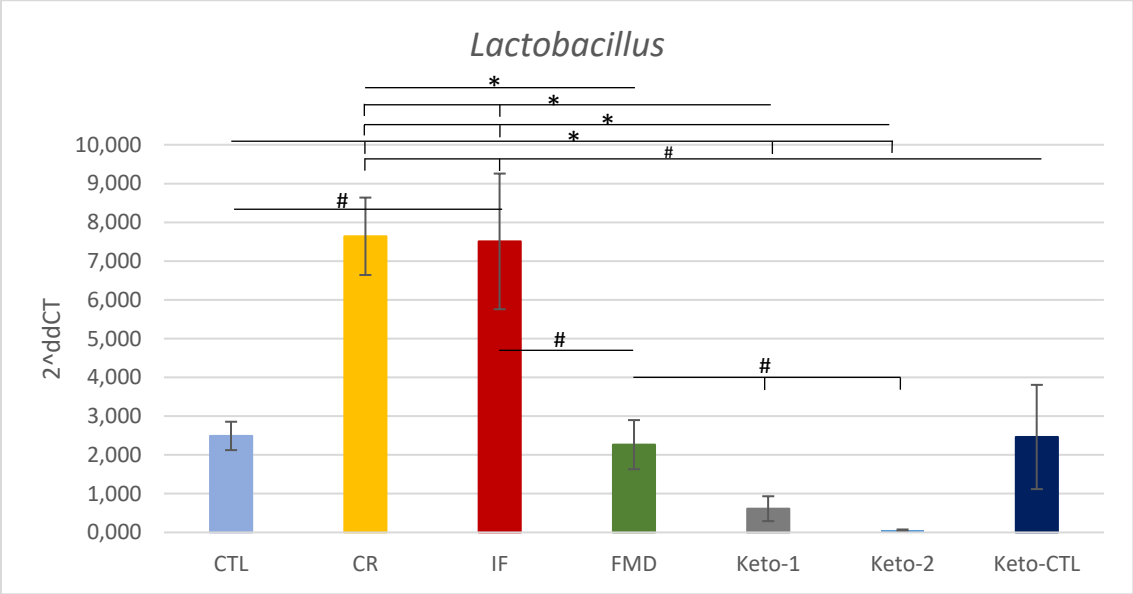

Figure 25: Gene analysis of Lactobacillus in small intestine epithelium tissue

5.5.5 DNA analysis of *Firmicutes* in the feces

Regarding the DNA analysis of *Firmicutes* in the feces, the Keto-1 mice showed by far the lowest number of these bacteria. The difference of this group compared to the CR, IF and FMD groups was statistically significant *(p ≤ 0,0071*) and a strong trend was measured between the Keto-1 group compared to the Keto-2 *(p = 0,010)* and Keto-CTL (p=0,043) groups. The increase of the bacteria number in the IF group compared to the Keto-2 (p=0,017) and Keto-CTL groups *(p = 0,013)* showed a strong trend as well as the increase in the IF (p=0,021) and FMD mice (p=0,023) compared to the CR mice. Last, the stronger expressed Firmicutes population in the FMD group showed a strong trend compared to the Keto-2 (p=0,021) and Keto-CTL groups (p=0,016).

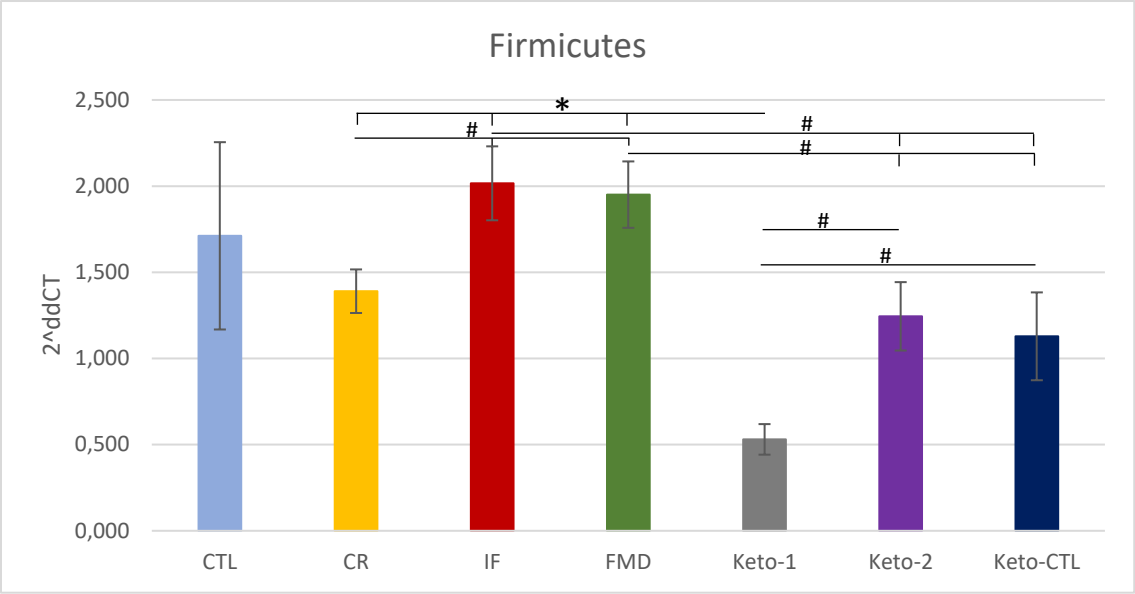

Figure 26: Gene analysis of Firmicutes in small intestine epithelium tissue

5.5.6 DNA analysis of Streptococcus in the feces

By analysis of the bacteria Streptococcus, the Keto-CTL mice had the highest bacteria number in the feces, followed by Keto-2 mice. The difference between the Keto-CTL mice compared to the CTL, CR, IF, FMD and Keto-1 mice was statistically significant *($p \leq 0{,}0071$)*. Although the Keto-2 mice showed also a high abundance, the deviations were too high for any significances.

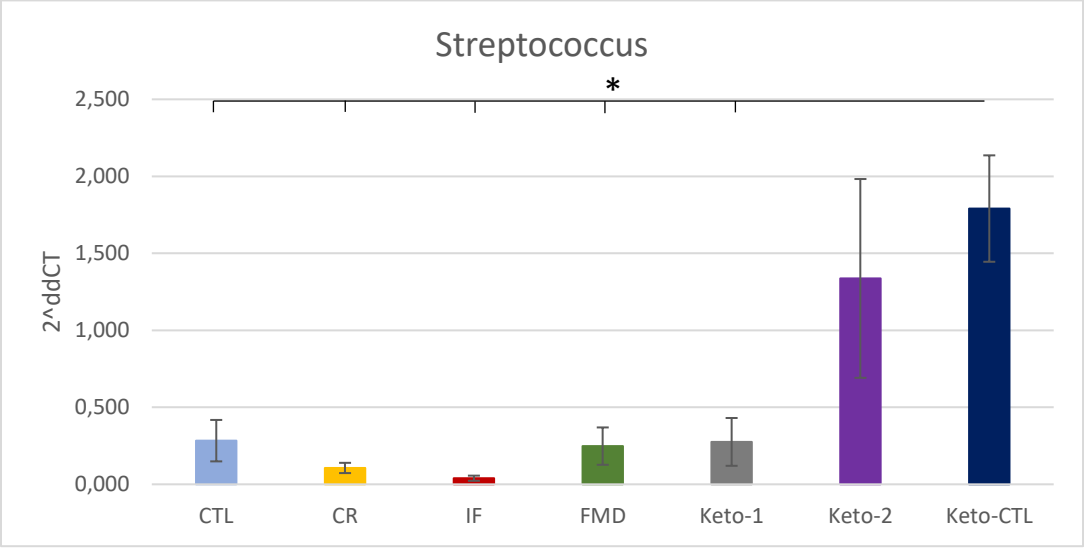

Figure 27: Gene analysis of Streptococcus in small intestine epithelium tissue

5.6 Protein arrays for the small intestine epithelium tissue

To investigate the effect of different diets on the immune response, the expression of 16 cytokines were measured with a protein array. No statistically significant differences were measured.

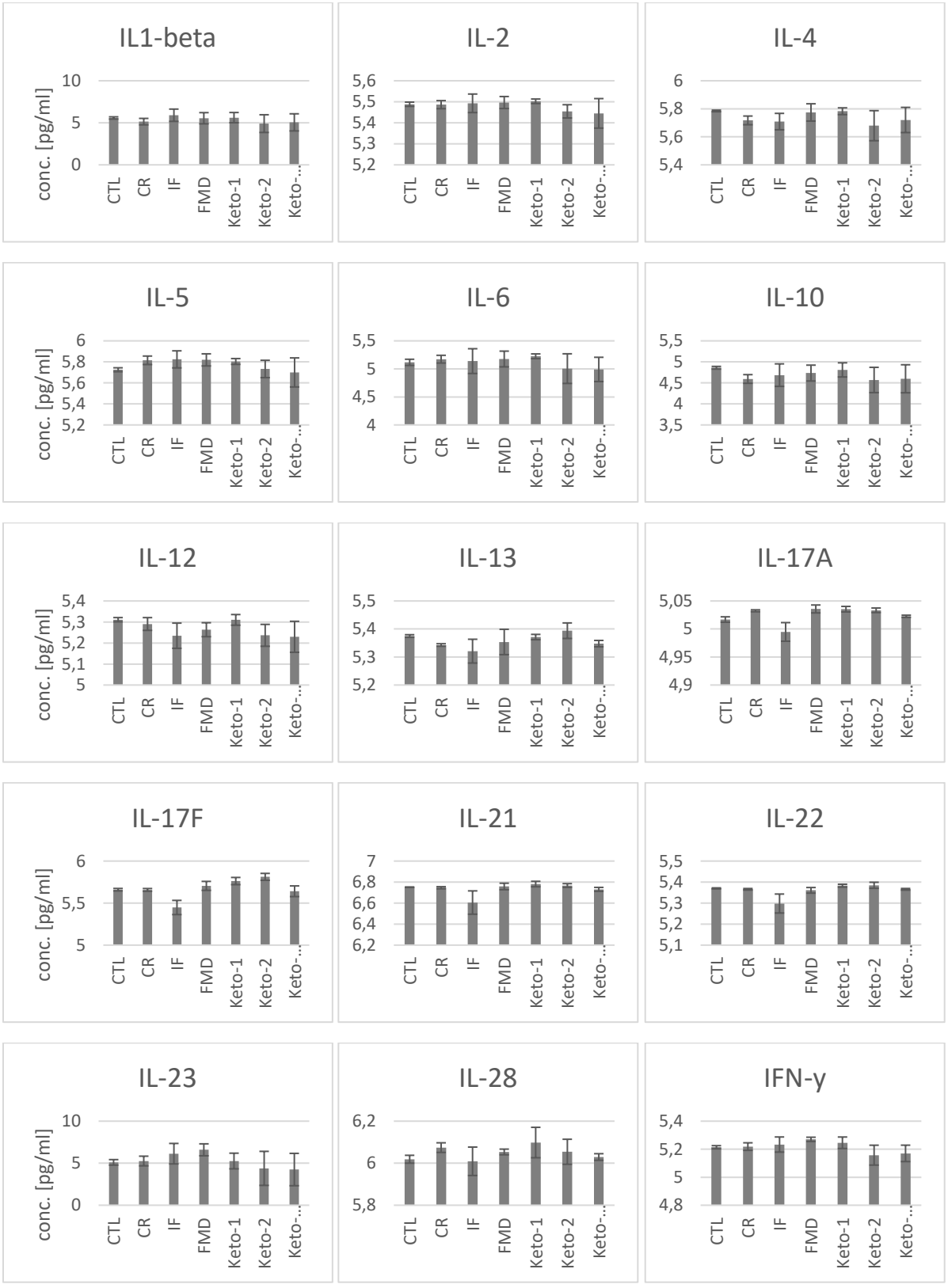

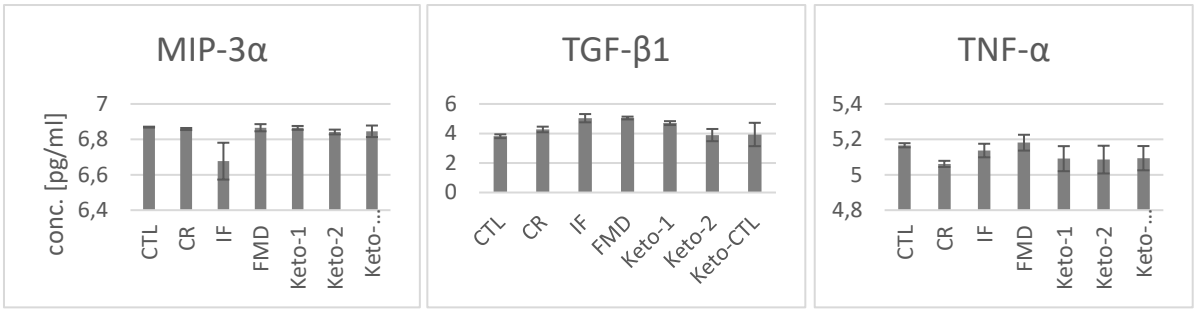

Figure 28: Cytokine expression in the small intestine epithelium tissue. Concentration (conc.), interleukin (IL), interferon gamma (IFN-γ), macrophage inflammatory protein (MIP-3α), Transforming growth factor β 1 (TGF-β1), tumor necrosis factor α (TNF- α).

6. Discussion

This study showed that restrictive diets had a positive impact on different inflammation markers in the gastrointestinal tract.

A higher *Parasutterella* number in the gastrointestinal tract was associated with protection from infections due to the metabolic end product succinate, which is produced by these bacteria. In a previous study it was shown, that succinate stimulated the colonization of anaerobic bacteria that in further consequence improved the immune function in mice [61]. Therefore, an increased number of *Parasutterella* in the feces, as it was measured for the CR mice, could have a positive impact on microbial interactions and the immune response. The Keto-2 and Keto-CTL mice showed compared to the other diets a low number of Parasutterella. Some values of the bacteria from the FMD group were higher compared to the other diet groups, but because of the small sample number of eight mice, no significant differences could be measured. Further experiments for the FMD group regarding the *Parasutterella* abundance in the gastrointestinal tract are suggested.
Like *Parasutterella*, also *Streptococcus* showed a better impact of the bacteria composition in the FMD, CR, IF and Keto-1 groups compared to the Keto-2 and Keto-CTL groups. These last two diet groups showed by far the highest abundance of these bacteria in the feces. Previous studies associated an abundance of this population with low grade inflammation [9] and chronic skin diseases [99].
And also the investigation of *Deferribacter, Bacteroidetes* and *Lactobacillus* support the theory that the CR, IF and FMD diets have a better impact on the microbiota composition compared to the ketogenic diets, especially the Keto-2 group.
In this study, higher numbers of *Deferribacter* were measured for some values of the Keto-1 and Keto-2 mice compared to the CR, IF and FMD mice. In a recent study from León et al. an increase of *Deferribacter* population in the gastrointestinal tract was associated with inflammatory metabolic pathways such as higher expressions of proinflammatory cytokines, especially in the colonic mucosa [68].
Having a look at the *Bacteroidetes* levels in the feces, some values of the ketogenic diets were lower compared to the FMD, CR and IF diets. Especially the decrease of the Keto-2 mice compared to the CR mice showed a strong trend. In previous experiments, an abundance of *Bacteroidetes* in the gastrointestinal tract was associated with a decrease in LDL-Cholesterol [92]. A decrease of the population, however, was associated with obesity [72] and chronic inflammatory skin diseases. In this study, the CR mice showed the most beneficial impact on the *Bacteroidetes* population in the feces.
The caloric restricted but carbohydrate rich diets CR and IF showed the highest *Lactobacillus* expression in the feces, the Keto-2 diet the lowest. A depletion of *Lactobacillus* was in previous studies associated with diverse inflammatory diseases [1, 15, 34, 75, 115, 122, 130]. Contrary to our findings, Ma et al. showed that 12- to 14-week-old healthy mice fed with a ketogenic diet had a significant increase in *Lactobacillus* levels compared to the control group [79]. This effect could not be observed in this study.

Regarding *Firmicutes*, statistically significantly lower levels of these bacteria in the feces were observed in the Keto-1 diet. The Keto-2 diet however, had a similar abundance like the other

carbohydrate rich restrictive diets, although it had the same fat percentage as the Keto-1 diet, just another composition. This study showed that a diet consisting of LCTs with a simultaneous decrease of carbohydrates resulted in the lowest fecal *Firmicutes* levels. Previous examinations associated a lower number of *Firmicutes* in the gastrointestinal tract with the prevention of weight gain and obesity [50, 81, 105]. Based on these findings, the Keto-1 mice showed the most positive impact on the *Firmicutes* population in this study. Changing the fat composition from LCTs to LCTs and MCTs, the positive impact vanished. It is known that *Firmicutes* are well suited to grow on carbohydrates [112]. In this experiment the carbohydrate rich diets CTL, CR, IF, FMD, Keto-CTL as well as Keto-2 diet showed a higher number of *Firmicutes* in the feces compared to the Keto-1 diet. Consequently, the fat source as well as the carbohydrate content played a crucial role in the abundance of these bacteria.

To summarize the results of the fecal bacteria, this experiment indicated, that the FMD, CR and IF diets had the best impact on the bacteria composition in the feces, the Keto-2 diet however the worst, especially regarding *Parasutterella, Lactobacillus* and *Streptococcus* expression. Consequently, the food composition played a crucial role in the number of different gastrointestinal microbiota. Due to the fact, that the bacteria mainly use components in carbohydrates as food sources, the biggest differences are apparent between carbohydrate-rich and carbohydrate-low diets. Based on this data, the carbohydrate rich restrictive diets FMD, CR and IF had a stronger positive impact on the gastrointestinal microbiota compared to the ketogenic diets, whereby the Keto-1 group with LCTs as fat source showed better results than the Keto-2 group with LCTs and MCTs. A study from Paoli et al. supports our findings that the fat constitution plays a crucial role in the composition of the microbiota [98].

Having a look at the cross-sections of small intestine and colon, the biggest differences were measured between the ketogenic diets and the other restrictive diets. The results of the crypt examinations in the colon showed a strong trend of a decrease in crypt depth in the Keto-2 mice compared to the other diet groups. In previous studies, inflammatory processes in the gastrointestinal tract were characterized by reduced villous length and crypt depth, atrophy and disruption [17, 104, 123]. These results in the Keto-2 group may be due to the more inflammatory bacterial composition compared to the other diet groups. In contrast, in cross-sections of the small intestine, the Keto-1 and Keto-2 mice showed a strong trend towards an increase in villous length. The shorter crypt depth in the colon on the one hand, and increased villous length in the small intestine on the other, could be explained by the different microbiota colonization in the intestine. Bacteria reach the highest cell density in the colon [111]. Therefore, changes in the microbiota could have the greatest effects in the colon. Compared to Blackmore et al., this thesis did not show that a higher food intake resulted in increased villous height and crypt depth [6]. In this experiment, no increased villous length and crypt depth were measured between the CTL mice and the other groups. Only the Keto-1 and Keto-2 groups showed higher values of the villous length in the small intestine.

Like the results of Fernandez-Estivariz et al., no visible changes in goblet cell numbers in the colon were measured by restrictive diets in this study [28]. Only in the Keto-2 group with mixed LCTs and MCTs was a lower number of mucin-secreting cells found. Further research in this area is needed to substantiate these findings.

If you pass the first epithelial layer and look at the muscularis externa, lower values for the thickness of the muscularis externa were measured in both the small intestine and colon on all restrictive diets, especially the ketogenic diets. Changes in the muscularis externa have been explained in previous experiments by an activation of macrophages and a subsequent release of chemokines and cytokines, which cause an inflammatory cell influx of immune cells such as neutrophil granulocytes and mononuclear cells. Subsequently, the morphology and homeostatic functionality of the muscularis externa changes [125]. The thicker the muscle, the more immune cells are activated.

Regarding the expression of IkBα in the small intestine epithelium tissue, a strong trend of an increase was measured for the IF, FMD, Keto-1 and Keto-2 mice. Higher IkBα levels have an anti-inflammatory effect because of the inhibition of the proinflammatory transcription factor NF-kB [74]. Previous studies described a decrease in IkBα and an increase of NF-kB and proinflammatory cytokines by diverse inflammatory processes [5, 21, 86]. This study showed that restrictive diets had a beneficial impact on the IkBα expression in the small intestine epithelium tissue and therefore on the immune regulation in the body. This theory is also supported by a study from Zhang et al. which represented, that CR was associated with a reduction in oxidative and inflammatory stress and retarded cell senescence through the suppressing of NF-kB pathway [5, 135]. This experiment serves as a fundament for further investigations to concretize and specify these findings.

Contrary to previous studies, no alterations in cytokine levels were measured in our experiment. Zhang et al. showed a lower IL-1ß expression in CR [135]. Other studies described the correlation between a decrease in IkBα and an increase in the expression of proinflammatory cytokines such as TNF-a, IL-12 and IL-18 [5, 21, 86]. In this experiment, however, no associations between increased IkBα levels and decreased proinflammatory cytokine levels in the small intestine epithelium tissue were measured. Notably is, that the Peyer's patches were removed before the measurement. Therefore, most of the immune cells from the small intestine epithelium tissue were not included. Another experiment with Peyer's patches included is suggested.

Both antioxidative enzymes GSTA3 and MGST1 showed an increase in mRNA expression in the small intestine epithelium tissue upon the restrictive diets, especially in the Keto-1 diet. A higher GSTA3 and MGST1 expression in the small intestine epithelium tissue leads to a higher concentration of antioxidants, less oxidative stress and a reduction of gastrointestinal inflammation [3, 4]. Because of the greatest expression observed in the Keto-1 mice intestine, these results show that a high concentration of LCTs with a simultaneous decrease of carbohydrates boosts the gene expression of GSTA3 and MGST1 the most. Modifications in the fatty acid composition change membrane fluidity and cell signaling what consequently leads to an altered gene expression [12]. Also, in this experiment, a change in fatty acid composition between the Keto-1 and Keto-2 mice led to changes in gene expression in the epithelium in the small intestine.

No changes in the gene expression of the two autophagy markers ATG7 and ATG12 were measured in the small intestine epithelium tissue in this study. Especially CR was described as a strong physiologically autophagy inducer [80, 106]. One explanation for our contrary results could be a statement from Chung et al., who said that it is challenging to implement autophagy, even by short-term CR [16]. A study from Derous et al. showed that a four-months CR intervention resulted in a significant increase in autophagy by male C57BL/6 mice [22]. Based on these findings, a longer CR intervention on male C57BL/6 mice is suggested.

7. Conclusion

This study showed that restrictive diets have an anti-inflammatory impact on the gastrointestinal tract in mice. Especially the diets CR, IF, FMD and Keto-1 were associated with a reduction in inflammation markers in the small intestine epithelium tissue.

Furthermore, the FMD, CR and IF mice showed a better impact on the microbiota composition in the feces compared to the ketogenic diets. Particularly in the Keto-2 group the microbiota composition altered in a more proinflammatory way compared to the other restrictive diets. By measurements of inflammation markers in the small intestine epithelium tissue and histological investigations of early ileum and colon, however, these differences vanished, except the decreased crypt depth in the colon in the Keto-2 mice. Therefore, based on this data, it cannot be concluded, which of the diets had the best effect on the microbiota composition and the inflammation markers in the intestine. Differences and indications regarding a reduction of inflammation levels in the intestine can only be formulated for the Keto-1 and Keto-2 mice. The Keto-1 mice showed thereby better results regarding the microbiota composition, several inflammation markers as well as morphological alterations compared to the Keto-2 mice. Therefore, in this experiment LCTs had a greater anti-inflammatory impact on the intestine than LCTs mixed with MCTs.

Restrictive diets promote coordinated effects on the organism instead of inhibiting just specific enzymes, as it is the case in most drugs for example. The range of restrictive diets goes from a daily calorie reduction (CR) to defined time slots of feeding during a day or feeding every other day (IF), undergoing periodic cycles of diets which can mimic several positive effects of fasting (FMD) or changing the food composition in a way of increasing the fat intake and decreasing the carbohydrate intake (Keto-diets). As the gastrointestinal tract is a key point for overall health, further investigations on what makes up diets which reduce gastrointestinal inflammation and optimize health span should be executed. There is a great potential in restrictive diets to counteract the development of chronic metabolic diseases like NCD and increase health and longevity. Additionally, these diets can be easily integrated into the medical care system as a cheap and simple way for improving health.

Therefore, this thesis is a great fundament for further investigations in gastrointestinal health.

8 References

[1] Alkanani, A. K., Hara, N., Gottlieb, P. A., Ir, D., Robertson, C. E., Wagner, B. D., Frank, D. N., and Zipris, D. 2015. Alterations in Intestinal Microbiota Correlate With Susceptibility to Type 1 Diabetes. *Diabetes* 64, 10, 3510–3520.

[2] Atreya, I., Atreya, R., and Neurath, M. F. 2008. NF-kappaB in inflammatory bowel disease. *Journal of internal medicine* 263, 6, 591–596.

[3] Bethesda. 2004. *National Library of Medicine (US), National Center for Biotechnology Information*. *glutathione S-transferase alpha 3 (GSTA3)*. https:// www.ncbi.nlm.nih.gov/gene/2940. Accessed 13 March 2021.

[4] Bethesda. 2012. *National Library of Medicine (US), National Center for Biotechnology Information*. *microsomal glutathione S-transferase 1 (MGST1)*. https://www.ncbi.nlm.nih.gov/ gene?Db=gene&Cmd=DetailsSearch&Term=4257. Accessed 6 March 2021.

[5] Biobaku, F., Ghanim, H., Batra, M., and Dandona, P. 2019. Macronutrient-Mediated Inflammation and Oxidative Stress: Relevance to Insulin Resistance, Obesity, and Atherogenesis. *J Clin Endocrinol Metab* 104, 12, 6118–6128.

[6] Blackmore, K., Zhou, W., and Dailey, M. J. 2017. LKB1-AMPK modulates nutrient-induced changes in the mode of division of intestinal epithelial crypt cells in mice. *Experimental biology and medicine (Maywood, N.J.)* 242, 15, 1490–1498.

[7] Blondhein, S. H., Horne, T., Kaufmann, N. A., and Rozen, P. 1981. Comparison of weight loss on low-calorie (800-1200) and very-low-calorie (300-600) diets. *International journal of obesity* 5, 3, 313–317.

[8] Board, P. G. and Menon, D. 2013. Glutathione transferases, regulators of cellular metabolism and physiology. *Biochimica et biophysica acta* 1830, 5, 3267–3288.

[9] Boer, C. G., Radjabzadeh, D., Medina-Gomez, C., Garmaeva, S., Schiphof, D., Arp, P., Koet, T., Kurilshikov, A., Fu, J., Ikram, M. A., Bierma-Zeinstra, S., Uitterlinden, A. G., Kraaij, R., Zhernakova, A., and van Meurs, Joyce B. J. 2019. Intestinal microbiome composition and its relation to joint pain and inflammation. *Nature communications* 10, 1, 4881.

[10] Borges-Canha, M., Portela-Cidade, J. P., Dinis-Ribeiro, M., Leite-Moreira, A. F., and Pimentel-Nunes, P. 2015. Role of colonic microbiota in colorectal carcinogenesis: a systematic review. *Revista espanola de enfermedades digestivas : organo oficial de la Sociedad Espanola de Patologia Digestiva* 107, 11, 659–671.

[11] Cabo, R. de and Mattson, M. P. 2019. Effects of Intermittent Fasting on Health, Aging, and Disease. *The New England journal of medicine* 381, 26, 2541–2551.

[12] Calder, P. C. 2012. Long-chain fatty acids and inflammation. *Proceedings of the Nutrition Society* 71, 2, 284–289.

[13] Campbell, M. K. and Farrell, S. O. 2006. *Biochemistry*. Brooks/Cole; Thomson Learning, Belmont, Calif., London.

[14] Caramés, B., Hasegawa, A., Taniguchi, N., Miyaki, S., Blanco, F. J., and Lotz, M. 2012. Autophagy activation by rapamycin reduces severity of experimental osteoarthritis. *Annals of the rheumatic diseases* 71, 4, 575–581.

[15] Chen, J., Chia, N., Kalari, K. R., Yao, J. Z., Novotna, M., Paz Soldan, M. M., Luckey, D. H., Marietta, E. V., Jeraldo, P. R., Chen, X., Weinshenker, B. G., Rodriguez, M., Kantarci, O. H., Nelson, H., Murray, J. A., and Mangalam, A. K. 2016. Multiple sclerosis patients have a distinct gut microbiota compared to healthy controls. *Scientific reports* 6, 28484.

[16] Chung, K. W. and Chung, H. Y. 2019. The Effects of Calorie Restriction on Autophagy: Role on Aging Intervention. *Nutrients* 11, 12, 2923.

[17] Ciaccio, E. J., Bhagat, G., Tennyson, C. A., Lewis, S. K., Hernandez, L., and Green, P. H. R. 2011. Quantitative assessment of endoscopic images for degree of villous atrophy in celiac disease. *Digestive diseases and sciences* 56, 3, 805–811.

[18] Clevers, H. 2013. The Intestinal Crypt, A Prototype Stem Cell Compartment. *Cell* 154, 2, 274–284.

[19] Cunnane, S., Nugent, S., Roy, M., Courchesne-Loyer, A., Croteau, E., Tremblay, S., Castellano, A., Pifferi, F., Bocti, C., Paquet, N., Begdouri, H., Bentourkia, M., Turcotte, E., Allard, M., Barberger-Gateau, P., Fulop, T., and Rapoport, S. I. 2011. Brain fuel metabolism, aging, and Alzheimer's disease. *Nutrition (Burbank, Los Angeles County, Calif.)* 27, 1, 3–20.

[20] Cunnane, S. C., Trushina, E., Morland, C., Prigione, A., Casadesus, G., Andrews, Z. B., Beal, M. F., Bergersen, L. H., Brinton, R. D., La Monte, S. de, Eckert, A., Harvey, J., Jeggo, R., Jhamandas, J. H., Kann, O., La Cour, C. M., Martin, W. F., Mithieux, G., Moreira, P. I., Murphy, M. P., Nave, K.-A., Nuriel, T., Oliet, S. H. R., Saudou, F., Mattson, M. P., Swerdlow, R. H., and Millan, M. J. 2020. Brain energy rescue: an emerging therapeutic concept for neurodegenerative disorders of ageing. *Nature reviews. Drug discovery* 19, 9, 609–633.

[21] Deopurkar, R., Ghanim, H., Friedman, J., Abuaysheh, S., Sia, C. L., Mohanty, P., Viswanathan, P., Chaudhuri, A., and Dandona, P. 2010. Differential effects of cream, glucose, and orange juice on inflammation, endotoxin, and the expression of Toll-like receptor-4 and suppressor of cytokine signaling-3. *Diabetes care* 33, 5, 991–997.

[22] Derous, D., Mitchell, S. E., Wang, L., Green, C. L., Wang, Y., Chen, L., Han, J.-D. J., Promislow, D. E. L., Lusseau, D., Douglas, A., and Speakman, J. R. 2017. The effects of graded levels of calorie restriction: XI. Evaluation of the main hypotheses underpinning the life extension effects of CR using the hepatic transcriptome. *Aging* 9, 7, 1770–1824.

[23] Donati, A., Cavallini, G., and Bergamini, E. 2013. Effects of aging, antiaging calorie restriction and in vivo stimulation of autophagy on the urinary excretion of 8OHdG in male Sprague-Dawley rats. *Age (Dordrecht, Netherlands)* 35, 2, 261–270.

[24] Drissi, F., Raoult, D., and Merhej, V. 2017. Metabolic role of lactobacilli in weight modification in humans and animals. *Microbial pathogenesis* 106, 182–194.

[25] Eckmann, L., Jung, H. C., Schürer-Maly, C., Panja, A., Morzycka-Wroblewska, E., and Kagnoff, M. F. 1993. Differential cytokine expression by human intestinal epithelial cell lines: regulated expression of interleukin 8. *Gastroenterology* 105, 6, 1689–1697.

[26] Faust, K., Sathirapongsasuti, J. F., Izard, J., Segata, N., Gevers, D., Raes, J., and Huttenhower, C. 2012. Microbial Co-occurrence Relationships in the Human Microbiome. *PLoS Computational Biology* 8, 7.

[27] Fellows, R. and Varga-Weisz, P. 2019. Chromatin dynamics and histone modifications in the intestinal microbiota-host crosstalk. *Molecular Metabolism* 38.

[28] Fernandez-Estivariz, C., Gu, L. H., Gu, L., Jonas, C. R., Wallace, T. M., Pascal, R. R., Devaney, K. L., Farrell, C. L., Jones, D. P., Podolsky, D. K., and Ziegler, T. R. 2003. Trefoil peptide expression and goblet cell number in rat intestine: effects of KGF and fasting-refeeding. *American journal of physiology. Regulatory, integrative and comparative physiology* 284, 2, R564-73.

[29] Fiocchi, C. 1998. Inflammatory bowel disease: etiology and pathogenesis. *Gastroenterology* 115, 1, 182–205.

[30] Fonseca, D. M. d., Hand, T. W., Han, S.-J., Gerner, M. Y., Glatman Zaretsky, A., Byrd, A. L., Harrison, O. J., Ortiz, A. M., Quinones, M., Trinchieri, G., Brenchley, J. M., Brodsky, I. E., Germain, R. N., Randolph, G. J., and Belkaid, Y. 2015. Microbiota-Dependent Sequelae of Acute Infection Compromise Tissue-Specific Immunity. *Cell* 163, 2, 354–366.

[31] Forslund, K., Hildebrand, F., Nielsen, T., Falony, G., Le Chatelier, E., Sunagawa, S., Prifti, E., Vieira-Silva, S., Gudmundsdottir, V., Pedersen, H. K., Arumugam, M., Kristiansen, K., Voigt, A. Y., Vestergaard, H., Hercog, R., Costea, P. I., Kultima, J. R., Li, J., Jørgensen, T., Levenez, F., Dore, J., Nielsen, H. B., Brunak, S., Raes, J., Hansen, T., Wang, J., Ehrlich, S. D., Bork, P., and Pedersen, O. 2015. Disentangling type 2 diabetes and metformin treatment signatures in the human gut microbiota. *Nature* 528, 7581, 262–266.

[32] Freeman, J. M., Kossoff, E. H., and Hartman, A. L. 2007. The ketogenic diet: one decade later. *Pediatrics* 119, 3, 535–543.

[33] Fukao, T., Lopaschuk, G. D., and Mitchell, G. A. 2004. Pathways and control of ketone body metabolism: on the fringe of lipid biochemistry. *Prostaglandins, leukotrienes, and essential fatty acids* 70, 3, 243–251.

[34] Goffau, M. C. de, Fuentes, S., van den Bogert, B., Honkanen, H., Vos, W. M. de, Welling, G. W., Hyöty, H., and Harmsen, H. J. M. 2014. Aberrant gut microbiota composition at the onset of type 1 diabetes in young children. *Diabetologia* 57, 8, 1569–1577.

[35] Golubeva, A. V., Crampton, S., Desbonnet, L., Edge, D., O'Sullivan, O., Lomasney, K. W., Zhdanov, A. V., Crispie, F., Moloney, R. D., Borre, Y. E., Cotter, P. D., Hyland, N. P., O'Halloran, K. D., Dinan, T. G., O'Keeffe, G. W., and Cryan, J. F. 2015. Prenatal stress-induced alterations in major physiological systems

correlate with gut microbiota composition in adulthood. *Psychoneuroendocrinology* 60, 58–74.

[36] Grek, C. L., Zhang, J., Manevich, Y., Townsend, D. M., and Tew, K. D. 2013. Causes and consequences of cysteine S-glutathionylation. *The Journal of biological chemistry* 288, 37, 26497–26504.

[37] Habold, C., Chevalier, C., Dunel-Erb, S., Foltzer-Jourdainne, C., Le Maho, Y., and Lignot, J.-H. 2004. Effects of fasting and refeeding on jejunal morphology and cellular activity in rats in relation to depletion of body stores. *Scandinavian journal of gastroenterology* 39, 6, 531–539.

[38] Han, Y.-M., Ramprasath, T., and Zou, M.-H. 2020. β-hydroxybutyrate and its metabolic effects on age-associated pathology. *Experimental & molecular medicine* 52, 4, 548–555.

[39] Hatley, O. J. D., Jones, C. R., Galetin, A., and Rostami-Hodjegan, A. 2017. Quantifying gut wall metabolism: methodology matters. *Biopharmaceutics & drug disposition* 38, 2, 155–160.

[40] Hayes, J. D., Flanagan, J. U., and Jowsey, I. R. 2005. Glutathione transferases. *Annual review of pharmacology and toxicology* 45, 51–88.

[41] Hieken, T. J., Chen, J., Hoskin, T. L., Walther-Antonio, M., Johnson, S., Ramaker, S., Xiao, J., Radisky, D. C., Knutson, K. L., Kalari, K. R., Yao, J. Z., Baddour, L. M., Chia, N., and Degnim, A. C. 2016. The Microbiome of Aseptically Collected Human Breast Tissue in Benign and Malignant Disease. *Scientific reports* 6, 30751.

[42] Hinz, M. and Scheidereit, C. 2014. The IκB kinase complex in NF-κB regulation and beyond. *EMBO reports* 15, 1, 46–61.

[43] Hirao, L. A., Grishina, I., Bourry, O., Hu, W. K., Somrit, M., Sankaran-Walters, S., Gaulke, C. A., Fenton, A. N., Li, J. A., Crawford, R. W., Chuang, F., Tarara, R., Marco, M. L., Bäumler, A. J., Cheng, H., and Dandekar, S. 2014. Early mucosal sensing of SIV infection by paneth cells induces IL-1β production and initiates gut epithelial disruption. *PLoS pathogens* 10, 8, e1004311.

[44] Hoesel, B. and Schmid, J. A. 2013. The complexity of NF-κB signaling in inflammation and cancer. *Molecular cancer* 12, 86.

[45] Hoffmann, A. and Baltimore, D. 2006. Circuitry of nuclear factor kappaB signaling. *Immunological reviews* 210, 171–186.

[46] Hu, H.-J., Park, S.-G., Jang, H. B., Choi, M.-K., Park, K.-H., Kang, J. H., Park, S. I., Lee, H.-J., and Cho, S.-H. 2015. Obesity Alters the Microbial Community Profile in Korean Adolescents. *PloS one* 10, 7, e0134333.

[47] Human Microbiome Project Consortium. 2012. Structure, function and diversity of the healthy human microbiome. *Nature* 486, 7402, 207–214.

[48] Huttenlocher, P. R., Wilbourn, A. J., and Signore, J. M. 1971. Medium-chain triglycerides as a therapy for intractable childhood epilepsy. *Neurology* 21, 11, 1097.

[49] Ignacio, A., Fernandes, M. R., Rodrigues, V. A. A., Groppo, F. C., Cardoso, A. L., Avila-Campos, M. J., and Nakano, V. 2016. Correlation between body mass index and faecal microbiota from children. *Clinical microbiology and infection : the official publication of the European Society of Clinical Microbiology and Infectious Diseases* 22, 3, 258.e1-8.

[50] Indiani, C. M. D. S. P., Rizzardi, K. F., Castelo, P. M., Ferraz, L. F. C., Darrieux, M., and Parisotto, T. M. 2018. Childhood Obesity and Firmicutes/Bacteroidetes Ratio in the Gut Microbiota: A Systematic Review. *Childhood obesity (Print)* 14, 8, 501–509.

[51] Israël, A. 2010. The IKK complex, a central regulator of NF-kappaB activation. *Cold Spring Harbor perspectives in biology* 2, 3, a000158.

[52] Jandhyala, S. M., Talukdar, R., Subramanyam, C., Vuyyuru, H., Sasikala, M., and Nageshwar Reddy, D. 2015. Role of the normal gut microbiota. *World journal of gastroenterology* 21, 29, 8787–8803.

[53] Janssen-Heininger, Y. M. W., Nolin, J. D., Hoffman, S. M., van der Velden, Jos L, Tully, J. E., Lahue, K. G., Abdalla, S. T., Chapman, D. G., Reynaert, N. L., van der Vliet, A., and Anathy, V. 2013. Emerging mechanisms of glutathione-dependent chemistry in biology and disease. *Journal of cellular biochemistry* 114, 9, 1962–1968.

[54] Jensen, N. J., Wodschow, H. Z., Nilsson, M., and Rungby, J. 2020. Effects of Ketone Bodies on Brain Metabolism and Function in Neurodegenerative Diseases. *International journal of molecular sciences* 21, 22.

[55] Jones, J. T., Qian, X., van der Velden, Jos L J, Chia, S. B., McMillan, D. H., Flemer, S., Hoffman, S. M., Lahue, K. G., Schneider, R. W., Nolin, J. D., Anathy, V., van der Vliet, A., Townsend, D. M., Tew, K. D., and Janssen-Heininger, Y. M. W. 2016. Glutathione S-transferase pi modulates NF-κB activation and pro-inflammatory responses in lung epithelial cells. *Redox biology* 8, 375–382.

[56] Kamada, N., Chen, G. Y., Inohara, N., and Núñez, G. 2013. Control of pathogens and pathobionts by the gut microbiota. *Nature immunology* 14, 7, 685–690.

[57] Kamdar, K., Khakpour, S., Chen, J., Leone, V., Brulc, J., Mangatu, T., Antonopoulos, D. A., Chang, E. B., Kahn, S. A., Kirschner, B. S., Young, G., and DePaolo, R. W. 2016. Genetic and Metabolic Signals during Acute Enteric Bacterial Infection Alter the Microbiota and Drive Progression to Chronic Inflammatory Disease. *Cell host & microbe* 19, 1, 21–31.

[58] Karakan, T. 2019. Intermittent fasting and gut microbiota. *The Turkish journal of gastroenterology : the official journal of Turkish Society of Gastroenterology* 30, 12, 1008.

[59] Karlsson, F. H., Tremaroli, V., Nookaew, I., Bergström, G., Behre, C. J., Fagerberg, B., Nielsen, J., and Bäckhed, F. 2013. Gut metagenome in European women with normal, impaired and diabetic glucose control. *Nature* 498, 7452, 99–103.

[60] Kim, Y. S. and Ho, S. B. 2010. Intestinal goblet cells and mucins in health and disease: recent insights and progress. *Current gastroenterology reports* 12, 5, 319–330.

[61] Kim, Y.-G., Sakamoto, K., Seo, S.-U., Pickard, J. M., Gillilland, M. G., Pudlo, N. A., Hoostal, M., Li, X., Wang, T. D., Feehley, T., Stefka, A. T., Schmidt, T. M., Martens, E. C., Fukuda, S., Inohara, N., Nagler, C. R., and Núñez, G. 2017. Neonatal acquisition of Clostridia species protects against colonization by bacterial pathogens. *Science (New York, N.Y.)* 356, 6335, 315–319.

[62] Kong, S., Zhang, Y. H., Zhang, W., and Ishihara, S. 2018. Regulation of Intestinal Epithelial Cells Properties and Functions by Amino Acids. *BioMed Research International* 2018, 2819154.

[63] Kossoff, E. H. and Wang, H.-S. 2013. Dietary therapies for epilepsy. *Biomedical journal* 36, 1, 2–8.

[64] Krebs, H. 1960. Biochemical Aspects of Ketosis. *Proceedings of the Royal Society of Medicine* 53, 2, 71–80.

[65] Landi, S. 2000. Mammalian class theta GST and differential susceptibility to carcinogens: a review. *Mutation research* 463, 3, 247–283.

[66] Lapébie, P., Lombard, V., Drula, E., Terrapon, N., and Henrissat, B. 2019. Bacteroidetes use thousands of enzyme combinations to break down glycans. *Nature communications* 10, 1, 2043.

[67] Le Roy, C. I., Štšepetova, J., Sepp, E., Songisepp, E., Claus, S. P., and Mikelsaar, M. 2015. New insights into the impact of Lactobacillus population on host-bacteria metabolic interplay. *Oncotarget* 6, 31, 30545–30556.

[68] León, I. C., Quesada-Vázquez, S., Sáinz, N., Guruceaga, E., Escoté, X., and Moreno-Aliaga, M. J. 2020. Effects of Maresin 1 (MaR1) on Colonic Inflammation and Gut Dysbiosis in Diet-Induced Obese Mice. *Microorganisms* 8, 8.

[69] Lessan, N. and Ali, T. 2019. Energy Metabolism and Intermittent Fasting: The Ramadan Perspective. *Nutrients* 11, 5, 1192.

[70] Lewis, J. D., Chen, E. Z., Baldassano, R. N., Otley, A. R., Griffiths, A. M., Lee, D., Bittinger, K., Bailey, A., Friedman, E. S., Hoffmann, C., Albenberg, L., Sinha, R., Compher, C., Gilroy, E., Nessel, L., Grant, A., Chehoud, C., Li, H., Wu, G. D., and Bushman, F. D. 2015. Inflammation, Antibiotics, and Diet as Environmental Stressors of the Gut Microbiome in Pediatric Crohn's Disease. *Cell host & microbe* 18, 4, 489–500.

[71] Ley, R. E., Hamady, M., Lozupone, C., Turnbaugh, P. J., Ramey, R. R., Bircher, J. S., Schlegel, M. L., Tucker, T. A., Schrenzel, M. D., Knight, R., and Gordon, J. I. 2008. Evolution of mammals and their gut microbes. *Science (New York, N.Y.)* 320, 5883, 1647–1651.

[72] Ley, R. E., Turnbaugh, P. J., Klein, S., and Gordon, J. I. 2006. Microbial ecology: human gut microbes associated with obesity. *Nature* 444, 7122, 1022–1023.

[73] Li, G., Xie, C., Lu, S., Nichols, R. G., Tian, Y., Li, L., Patel, D., Ma, Y., Brocker, C. N., Yan, T., Krausz, K. W., Xiang, R., Gavrilova, O., Patterson, A. D., and Gonzalez, F. J. 2017. Intermittent Fasting Promotes White Adipose Browning and Decreases Obesity by Shaping the Gut Microbiota. *Cell metabolism* 26, 4, 672-685.e4.

[74] Liang, W.-J., Yang, H.-W., Liu, H.-N., Qian, W., and Chen, X.-L. 2020. HMGB1 upregulates NF-kB by inhibiting IKB-α and associates with diabetic retinopathy. *Life sciences* 241, 117146.

[75] Liu, H.-N., Wu, H., Chen, Y.-Z., Chen, Y.-J., Shen, X.-Z., and Liu, T.-T. 2017. Altered molecular signature of intestinal microbiota in irritable bowel syndrome patients compared with healthy controls: A systematic review and meta-analysis. *Digestive and liver disease : official journal of the Italian Society of Gastroenterology and the Italian Association for the Study of the Liver* 49, 4, 331–337.

[76] Liu, X., Zeng, B., Zhang, J., Li, W., Mou, F., Wang, H., Zou, Q., Zhong, B., Wu, L., Wei, H., and Fang, Y. 2016. Role of the Gut Microbiome in Modulating Arthritis Progression in Mice. *Scientific reports* 6, 30594.

[77] Longo, V. D. and Panda, S. 2016. Fasting, circadian rhythms, and time restricted feeding in healthy lifespan. *Cell metabolism* 23, 6, 1048–1059.

[78] Lupp, C., Robertson, M. L., Wickham, M. E., Sekirov, I., Champion, O. L., Gaynor, E. C., and Finlay, B. B. 2007. Host-mediated inflammation disrupts the intestinal microbiota and promotes the overgrowth of Enterobacteriaceae. *Cell host & microbe* 2, 2, 119–129.

[79] Ma, D., Wang, A. C., Parikh, I., Green, S. J., Hoffman, J. D., Chlipala, G., Murphy, M. P., Sokola, B. S., Bauer, B., Hartz, A. M. S., and Lin, A.-L. 2018. Ketogenic diet enhances neurovascular function with altered gut microbiome in young healthy mice. *Sci Rep* 8, 1, 6670.

[80] Madeo, F., Zimmermann, A., Maiuri, M. C., and Kroemer, G. 2015. Essential role for autophagy in life span extension. *The Journal of clinical investigation* 125, 1, 85–93.

[81] Magne, F., Gotteland, M., Gauthier, L., Zazueta, A., Pesoa, S., Navarrete, P., and Balamurugan, R. 2020. The Firmicutes/Bacteroidetes Ratio: A Relevant Marker of Gut Dysbiosis in Obese Patients? *Nutrients* 12, 5.

[82] Meister, A. and Anderson, M. E. 1983. Glutathione. *Annual review of biochemistry* 52, 711–760.

[83] Michalsen, A. 2010. Prolonged fasting as a method of mood enhancement in chronic pain syndromes: a review of clinical evidence and mechanisms. *Current pain and headache reports* 14, 2, 80–87.

[84] Michalsen, A. and Li, C. 2013. Fasting Therapy for Treating and Preventing Disease - Current State of Evidence. *Complement Med Res* 20, 6, 444–453.

[85] Mikuda, N., Schmidt-Ullrich, R., Kärgel, E., Golusda, L., Wolf, J., Höpken, U. E., Scheidereit, C., Kühl, A. A., and Kolesnichenko, M. 2020. Deficiency in IκBα in the intestinal epithelium leads to spontaneous inflammation and mediates apoptosis in the gut. *The Journal of pathology* 251, 2, 160–174.

[86] Mohanty, P., Ghanim, H., Hamouda, W., Aljada, A., Garg, R., and Dandona, P. 2002. Both lipid and protein intakes stimulate increased generation of reactive oxygen species by polymorphonuclear leukocytes and mononuclear cells. *The American journal of clinical nutrition* 75, 4, 767–772.

[87] Møller, N. 2020. Ketone Body, 3-Hydroxybutyrate: Minor Metabolite - Major Medical Manifestations. *The Journal of clinical endocrinology and metabolism* 105, 9.

[88] Moritz, C. P. 2020. 40 years Western blotting: A scientific birthday toast. *Journal of Proteomics* 212, 103575.

[89] Neal, E. G., Chaffe, H., Schwartz, R. H., Lawson, M. S., Edwards, N., Fitzsimmons, G., Whitney, A., and Cross, J. H. 2008. The ketogenic diet for the treatment of childhood epilepsy: a randomised controlled trial. *The Lancet Neurology* 7, 6, 500–506.

[90] Neurath, M. F., Becker, C., and Barbulescu, K. 1998. Role of NF-kappaB in immune and inflammatory responses in the gut. *Gut* 43, 6, 856–860.

[91] Neurath, M. F., Pettersson, S., Meyer zum Büschenfelde, K H, and Strober, W. 1996. Local administration of antisense phosphorothioate oligonucleotides to the p65 subunit of NF-kappa B abrogates established experimental colitis in mice. *Nature medicine* 2, 9, 998–1004.

[92] Nuli, R., Cai, J., Kadeer, A., Zhang, Y., and Mohemaiti, P. 2019. Integrative Analysis Toward Different Glucose Tolerance-Related Gut Microbiota and Diet. *Frontiers in endocrinology* 10, 295.

[93] Omodei, D. and Fontana, L. 2011. Calorie restriction and prevention of age-associated chronic disease. *FEBS letters* 585, 11, 1537–1542.

[94] Osaka, T., Moriyama, E., Arai, S., Date, Y., Yagi, J., Kikuchi, J., and Tsuneda, S. 2017. Meta-Analysis of Fecal Microbiota and Metabolites in Experimental Colitic Mice during the Inflammatory and Healing Phases. *Nutrients* 9, 12.

[95] Ouwerkerk, J. P., Vos, W. M. de, and Belzer, C. 2013. Glycobiome: bacteria and mucus at the epithelial interface. *Best practice & research. Clinical gastroenterology* 27, 1, 25–38.

[96] Pagano, G., Niccolini, F., and Politis, M. 2016. Current status of PET imaging in Huntington's disease. *European journal of nuclear medicine and molecular imaging* 43, 6, 1171–1182.

[97] Panchuk-Voloshina, N., Haugland, R. P., Bishop-Stewart, J., Bhalgat, M. K., Millard, P. J., Mao, F., Leung, W.-Y., and Haugland, R. P. 1999. Alexa Dyes, a Series of New Fluorescent Dyes that Yield Exceptionally Bright, Photostable Conjugates. *Journal of Histochemistry & Cytochemistry* 47, 9, 1179–1188.

[98] Paoli, A., Mancin, L., Bianco, A., Thomas, E., Mota, J. F., and Piccini, F. 2019. Ketogenic Diet and Microbiota: Friends or Enemies? *Genes (Basel)* 10, 7, 534.

[99] Park, Y., Lee, S., Kang, M.-J., Kim, B.-S., Lee, M.-J., Jung, S., Yoon, J., Cho, H.-J., Lee, E., Yang, S.-I., Seo, J.-H., Kim, H.-B., Suh, D. I., Shin, Y., Ahn, K.-M., and Hong, S.-J. 2020. Imbalance of Gut Streptococcus , Clostridium , and Akkermansia Determines the Natural Course of Atopic Dermatitis in Infant. *Allergy, Asthma & Immunology Research* 12, 322.

[100] Patterson, R. E., Laughlin, G. A., LaCroix, A. Z., Hartman, S. J., Natarajan, L., Senger, C. M., Martínez, M. E., Villaseñor, A., Sears, D. D., Marinac, C. R., and Gallo, L. C. 2015. Intermittent Fasting and Human Metabolic Health. *Journal of the Academy of Nutrition and Dietetics* 115, 8, 1203–1212.

[101] Pearson, C., Uhlig, H. H., and Powrie, F. 2012. Lymphoid microenvironments and innate lymphoid cells in the gut. *Trends in immunology* 33, 6, 289–296.

[102] Petermann, A., Miene, C., Schulz-Raffelt, G., Palige, K., Hölzer, J., Glei, M., and Böhmer, F.-D. 2009. GSTT2, a phase II gene induced by apple polyphenols, protects colon epithelial cells against genotoxic damage. *Molecular nutrition & food research* 53, 10, 1245–1253.

[103] RayBiotech. 2019. *Quantibody Mouse TH17 Array 1*. *quantitative measurement of 18 mouse TH1-TH2-TH17 cytokines*. https://doc.raybiotech.com/pdf/Manual/QAM-TH17-1.pdf.

[104] Ritchie, J. M., Rui, H., Zhou, X., Iida, T., Kodoma, T., Ito, S., Davis, B. M., Bronson, R. T., and Waldor, M. K. 2012. Inflammation and disintegration of intestinal villi in an experimental model for Vibrio parahaemolyticus-induced diarrhea. *PLoS pathogens* 8, 3, e1002593.

[105] Riva, A., Borgo, F., Lassandro, C., Verduci, E., Morace, G., Borghi, E., and Berry, D. 2017. Pediatric obesity is associated with an altered gut microbiota and discordant shifts in Firmicutes populations. *Environmental microbiology* 19, 1, 95–105.

[106] Rubinsztein, D. C., Mariño, G., and Kroemer, G. 2011. Autophagy and aging. *Cell* 146, 5, 682–695.

[107] Sanderlin, E. J., Leffler, N. R., Lertpiriyapong, K., Cai, Q., Hong, H., Bakthavatchalu, V., Fox, J. G., Oswald, J. Z., Justus, C. R., Krewson, E. A., O'Rourke, E. A., and Yang, L. V. 2016. *GPR4 Deficiency Alleviates Intestinal Inflammation in a Mouse Model of Inflammatory Bowel Disease* 7.

[108] Schneeberger, E. E. and Lynch, R. D. 2004. The tight junction: a multifunctional complex. *American journal of physiology. Cell physiology* 286, 6, C1213-28.

[109] Schreiber, S., Nikolaus, S., and Hampe, J. 1998. Activation of nuclear factor kappa B inflammatory bowel disease. *Gut* 42, 4, 477–484.

[110] Schwiertz, A., Taras, D., Schäfer, K., Beijer, S., Bos, N. A., Donus, C., and Hardt, P. D. 2010. Microbiota and SCFA in lean and overweight healthy subjects. *Obesity (Silver Spring, Md.)* 18, 1, 190–195.

[111] Sender, R., Fuchs, S., and Milo, R. 2016. Revised Estimates for the Number of Human and Bacteria Cells in the Body. *PLoS biology* 14, 8, e1002533.

[112] Sharmin, F., Wakelin, S., Huygens, F., and Hargreaves, M. 2013. Firmicutes dominate the bacterial taxa within sugar-cane processing plants. *Sci Rep* 3, 1, 3107.

[113] Shintani, H., Shintani, T., Ashida, H., and Sato, M. 2018. Calorie Restriction Mimetics: Upstream-Type Compounds for Modulating Glucose Metabolism. *Nutrients* 10, 12.

[114] Sommer, F. and Bäckhed, F. 2013. The gut microbiota--masters of host development and physiology. *Nature reviews. Microbiology* 11, 4, 227–238.

[115] Stanisavljević, S., Lukić, J., Soković, S., Mihajlovic, S., Mostarica Stojković, M., Miljković, D., and Golić, N. 2016. Correlation of Gut Microbiota Composition with Resistance to Experimental Autoimmune Encephalomyelitis in Rats. *Frontiers in microbiology* 7, 2005.

[116] Talapka, P., Berkó, A., Nagy, L. I., Chandrakumar, L., Bagyánszki, M., Puskás, L. G., Fekete, É., and Bódi, N. 2016. Structural and molecular features of intestinal strictures in rats with Crohn's-like disease. *World journal of gastroenterology* 22, 22, 5154–5164.

[117] Tew, K. D. and Townsend, D. M. 2012. Glutathione-s-transferases as determinants of cell survival and death. *Antioxidants & redox signaling* 17, 12, 1728–1737.

[118] Tham, E. H. and Leung, D. Y. 2019. Mechanisms by Which Atopic Dermatitis Predisposes to Food Allergy and the Atopic March. *Allergy, Asthma & Immunology Research* 11, 1, 4–15.

[119] Tornatore, L., Thotakura, A. K., Bennett, J., Moretti, M., and Franzoso, G. 2012. The nuclear factor kappa B signaling pathway: integrating metabolism with inflammation. *Trends in cell biology* 22, 11, 557–566.

[120] Townsend, D. M. and Tew, K. D. 2003. The role of glutathione-S-transferase in anti-cancer drug resistance. *Oncogene* 22, 47, 7369–7375.

[121] Vandoorne, T., Bock, K. de, and van den Bosch, L. 2018. Energy metabolism in ALS: an underappreciated opportunity? *Acta neuropathologica* 135, 4, 489–509.

[122] Vujkovic-Cvijin, I., Swainson, L. A., Chu, S. N., Ortiz, A. M., Santee, C. A., Petriello, A., Dunham, R. M., Fadrosh, D. W., Lin, D. L., Faruqi, A. A., Huang, Y., Apetrei, C., Pandrea, I., Hecht, F. M., Pilcher, C. D., Klatt, N. R., Brenchley, J. M., Lynch, S. V., and McCune, J. M. 2015. Gut-Resident Lactobacillus Abundance Associates with IDO1 Inhibition and Th17 Dynamics in SIV-Infected Macaques. *Cell Reports* 13, 8, 1589–1597.

[123] Vyhlidal, C. A., Chapron, B. D., Ahmed, A., Singh, V., Casini, R., and Shakhnovich, V. 2021. Effect of Crohn's Disease on Villous Length and CYP3A4

Expression in the Pediatric Small Intestine. *Clinical and translational science* 14, 2, 729–736.

[124] Wang, W., Chen, L., Zhou, R., Wang, X., Song, L., Huang, S., Wang, G., and Xia, B. 2014. Increased proportions of Bifidobacterium and the Lactobacillus group and loss of butyrate-producing bacteria in inflammatory bowel disease. *Journal of clinical microbiology* 52, 2, 398–406.

[125] Wehner, S. and Engel, D. R. 2017. Resident macrophages in the healthy and inflamed intestinal muscularis externa. *Pflugers Archiv : European journal of physiology* 469, 3-4, 541–552.

[126] Willcox, B. J. and Willcox, D. C. 2014. Caloric restriction, caloric restriction mimetics, and healthy aging in Okinawa: controversies and clinical implications. *Curr Opin Clin Nutr Metab Care* 17, 1, 51–58.

[127] Willing, B. P., Dicksved, J., Halfvarson, J., Andersson, A. F., Lucio, M., Zheng, Z., Järnerot, G., Tysk, C., Jansson, J. K., and Engstrand, L. 2010. A pyrosequencing study in twins shows that gastrointestinal microbial profiles vary with inflammatory bowel disease phenotypes. *Gastroenterology* 139, 6, 1844-1854.e1.

[128] Wolters Kluwer Health. 2006. *Stedman's Medical Dictionary*. *Cytokine*. Williams & Wilkins, Lippincott.

[129] Xia, L., Yang, Y., Wang, J., Jing, Y., and Yang, Q. 2018. Impact of TGEV infection on the pig small intestine. *Virology journal* 15, 1, 102.

[130] Yang, L., Poles, M. A., Fisch, G. S., Ma, Y., Nossa, C., Phelan, J. A., and Pei, Z. 2016. HIV-induced immunosuppression is associated with colonization of the proximal gut by environmental bacteria. *AIDS* 30, 1.

[131] Yang, Y.-W., Chen, M.-K., Yang, B.-Y., Huang, X.-J., Zhang, X.-R., He, L.-Q., Zhang, J., and Hua, Z.-C. 2015. Use of 16S rRNA Gene-Targeted Group-Specific Primers for Real-Time PCR Analysis of Predominant Bacteria in Mouse Feces. *Applied and environmental microbiology* 81, 19, 6749–6756.

[132] Yoo, B. H., Khan, I. A., Koomson, A., Gowda, P., Sasazuki, T., Shirasawa, S., Gujar, S., and V. Rosen, K. 2017. Oncogenic RAS-induced downregulation of ATG12 is required for survival of malignant intestinal epithelial cells. *Autophagy* 14, 1, 134–151.

[133] Zelante, T., Iannitti, R. G., Cunha, C., Luca, A. de, Giovannini, G., Pieraccini, G., Zecchi, R., D'Angelo, C., Massi-Benedetti, C., Fallarino, F., Carvalho, A., Puccetti, P., and Romani, L. 2013. Tryptophan catabolites from microbiota engage aryl hydrocarbon receptor and balance mucosal reactivity via interleukin-22. *Immunity* 39, 2, 372–385.

[134] Zeng, M. Y., Inohara, N., and Nuñez, G. 2016. Mechanisms of inflammation-driven bacterial dysbiosis in the gut. *Mucosal immunology* 10, 1, 18–26.

[135] Zhang, N., Li, Z., Mu, W., Li, L., Liang, Y., Lu, M., Wang, Z., Qiu, Y., and Wang, Z. 2016. Calorie restriction-induced SIRT6 activation delays aging by suppressing NF-κB signaling. *Cell Cycle* 15, 7, 1009–1018.

[136] Zhang, X., Zhang, D., Jia, H., Feng, Q., Wang, D., Di Liang, Wu, X., Li, J., Tang, L., Li, Y., Lan, Z., Chen, B., Li, Y., Zhong, H., Xie, H., Jie, Z., Chen, W., Tang, S., Xu, X., Wang, X., Cai, X., Liu, S., Xia, Y., Li, J., Qiao, X., Al-Aama, J. Y., Chen, H., Wang, L., Wu, Q.-J., Zhang, F., Zheng, W., Li, Y., Zhang, M., Luo, G., Xue, W., Xiao, L., Li, J., Chen, W., Xu, X., Yin, Y., Yang, H., Wang, J., Kristiansen, K., Liu, L., Li, T., Huang, Q., Li, Y., and Wang, J. 2015. The oral and gut microbiomes are perturbed in rheumatoid arthritis and partly normalized after treatment. *Nature medicine* 21, 8, 895–905.

[137] Zheng, W., Xie, W., Yin, D., Luo, R., Liu, M., and Guo, F. 2019. ATG5 and ATG7 induced autophagy interplays with UPR via PERK signaling. *Cell Communication and Signaling : CCS* 17.

[138] Zijlmans, M. A. C., Korpela, K., Riksen-Walraven, J. M., Vos, W. M. de, and Weerth, C. de. 2015. Maternal prenatal stress is associated with the infant intestinal microbiota. *Psychoneuroendocrinology* 53, 233–245.

[139] Zilberter, Y. and Zilberter, M. 2017. The vicious circle of hypometabolism in neurodegenerative diseases: Ways and mechanisms of metabolic correction. *Journal of neuroscience research* 95, 11, 2217–2235.

[140] Zupec-Kania, B. A. and Spellman, E. 2008. An overview of the ketogenic diet for pediatric epilepsy. *Nutrition in clinical practice : official publication of the American Society for Parenteral and Enteral Nutrition* 23, 6, 589–596.